NASA TECHNICAL MEMORANDUM

NASA TM X-2659

NASA TM X-2659

FLOW CONDITIONS AROUND THE EXIT AND DOWNSTREAM OF CERTAIN STATOR BLADING WITH VARIOUS TRAILING-EDGE THICKNESSES AND GEOMETRIES

by Herman W. Prust, Jr. and Ronald M. Heiser

Lewis Research Center

Cleveland, Ohio 44135

NATIONAL AERONAUTICS AND SPACE ADMINISTRATION • WASHINGTON, D. C. • OCTOBER 1972

1. Report No.	2. Government Accession No.	3. Recipient's Catalog No.
NASA TM X-2659		

4. Title and Subtitle	5. Report Date
FLOW CONDITIONS AROUND THE EXIT AND DOWNSTREAM OF CERTAIN STATOR BLADING WITH VARIOUS TRAILING-EDGE THICKNESSES AND GEOMETRIES	October 1972
	6. Performing Organization Code

7. Author(s)	8. Performing Organization Report No.
Herman W. Prust, Jr., and Ronald M. Helon	E-7024
	10. Work Unit No. 764-74

9. Performing Organization Name and Address	11. Contract or Grant No.
Lewis Research Center National Aeronautics and Space Administration Cleveland, Ohio 44135	

12. Sponsoring Agency Name and Address	13. Type of Report and Period Covered
National Aeronautics and Space Administration Washington, D.C. 20546	Technical Memorandum
	14. Sponsoring Agency Code

15. Supplementary Notes

16. Abstract

The blading investigated was curved back with thick profiles. The variations in flow conditions considered were flow angle and isentropic energy. Experimental data were obtained in a two-dimensional cascade from surveys with a combined angle, total-, and static-pressure probe and from an array of end-wall static pressure taps. Analytical results were obtained from ideal flow theory. The results showed large variations in flow conditions close to the plane of the trailing-edge that were largely attenuated at a distance a little greater than one blade pitch downstream of the trailing edge in the direction of flow. The results were affected by the geometry and thickness of the trailing edge. The agreement between experimental and analytical results is generally fair to excellent.

17. Key Words (Suggested by Author(s))		18. Distribution Statement
Turbine	Trailing edge	Unclassified - unlimited
Blading	Analytical	
Stator	Experimental	
Flow conditions	Downstream	

19. Security Classif. (of this report)	20. Security Classif. (of this page)	21. No. of Pages	22. Price*
Unclassified	Unclassified	44	$3.00

* For sale by the National Technical Information Service, Springfield, Virginia 22151

FLOW CONDITIONS AROUND THE EXIT AND DOWNSTREAM OF CERTAIN STATOR BLADING WITH VARIOUS TRAILING-EDGE THICKNESSES AND GEOMETRIES

by Herman W. Prust, Jr., and Ronald M. Helon

Lewis Research Center

SUMMARY

An experimental and analytical investigation of the variations in flow conditions around the exit and downstream of certain curved back stator blading with thick profiles having round and square trailing edges of different thicknesses was conducted.

Experimental data were obtained in a two-dimensional cascade. Analytical results were obtained using an ideal-flow method developed at NASA Lewis.

The experimental results showed large variations in flow conditions in the trailing-edge plane for all the blades tested. These variations persisted for a distance of at least one-fourth blade pitch downstream of the blading in the direction of flow. Although slightly different, the large variations in flow conditions existed over the fairly wide range of fluid velocity levels investigated.

At a distance of approximately one blade pitch from the trailing-edge plane in the direction of flow, the variations in flow conditions were largely attenuated. In the trailing-edge plane, the variation in ideal specific kinetic energy, relative to the uniform ideal specific kinetic energy downstream of the blading was as large as about ±20 percent.

At a distance of about one-fourth of a blade pitch downstream of the blading, the variation in flow angle was about $\pm 4.5^{\circ}$.

The experimental results show that the static pressure at the blade trailing edge decreased significantly with increased trailing-edge thickness. This decrease in static pressure with increased trailing-edge thickness indicates a decrease in blade row efficiency. A decrease in blade row efficiency with increased trailing-edge thickness has been confirmed quantitatively by other investigations.

A comparison was made between experimentally and analytically determined variations in kinetic energy and flow angle. The agreement was excellent in many cases and fair in others. Considering the many possible reasons for differences between the experimental and analytical results, the agreement shown is perhaps better than might be expected. Among the reasons for expected differences is the fact that the analytical results are for an ideal fluid with no losses whereas the experimental results are for a real fluid with actual losses of the blade row.

INTRODUCTION

In cooled turbines, blading with thick profiles having curved backs are generally required to provide for internal coolant flow passages. Blade row loss is a function of the blade shape, including the trailing-edge thickness and trailing-edge geometry. Therefore, the flow conditions in the trailing-edge area that cause these losses are of interest. Besides, as reported in references 1 and 2, blade row losses based on pressure-loss measurements may be in error if the pressure-loss measurements are taken very close to the trailing edge. The evidence indicates that the error in blade-row loss results from large flow-angle and static-pressure variations and gradients in the wake region that cause errors in pressure-loss measurements and energy computations. Confirmation of these variations is therefore of interest.

Further, there are indications that rotor-blade-row losses are increased with increased flow variations at the rotor inlet (ref. 3). If so, it may be desirable to adjust the stator to rotor distance so that a proper compromise is reached between the loss due to the end wall and the loss due to flow variations.

For the reason given, an investigation of the flow conditions around the exit and downstream of certain stator blading with round and square trailing-edges of different thicknesses was undertaken. The investigation was conducted without coolant flow. The basic blading used is 10.16 centimeters (4.0 in.) high and has a chord of 5.74 centimeters (2.26 in.), a pitch of 4.14 centimeters (1.63 in.), and a nominal downstream turning angle of about 67° with axial flow at the inlet.

This investigation is an extension of the work of reference 4, using the same cascade and basic blading. Reference 4 reports the results of an investigation of the effect of different trailing-edge thicknesses and trailing-edge geometries on the efficiency of certain stator blading.

For the subject investigation, experimental data were obtained in a two-dimensional cascade. Flow angle data were obtained from surveys using a calibrated angle probe. Static pressures were determined both by surveys with a calibrated static-pressure probe and from an array of end-wall static pressure taps. Analytical data were obtained using the method of reference 5.

The results of the investigation are reported in terms of variations in flow angle and isentropic kinetic-energy ratios. (The isentropic kinetic energy ratio $\Delta H_{i,x}/\Delta H_{i,m}$ is the specific isentropic kinetic energy between total conditions at blade row inlet and the static pressure at any given location in the blade row divided by the specific isentropic kinetic energy between total conditions at blade row inlet and the uniform static pressure downstream of the blade row.) Experimental results are reported and compared with analytical results. In addition, comparisons of variations in isentropic energy ratios determined from wall-static-pressure-tap measurements and static-pressure-probe measurements are reported.

SYMBOLS

ΔH	specific energy difference between total and static conditions, J; Btu/lbm
$\frac{\Delta H_{i,x}}{\Delta H_{i,m}}$	ratio of specific isentropic kinetic energy between total conditions at blade row inlet and static pressure at any location in blade row to specific isentropic kinetic energy between total conditions at blade row inlet and uniform static pressure downstream of blade row
p	absolute pressure, N/m^2; lbf/ft^2
V	velocity, m/sec; ft/sec
γ	ratio of specific heats

Subscripts:

cr	conditions at Mach 1
i	isentropic process
m	uniform or mixed state downstream of blade row
x	any specified location in blade row
0	inlet conditions

Superscript:

'	total state

APPARATUS AND PROCEDURE

Cascade

The experimental investigation was conducted in a simple two-dimensional cascade (fig. 1). The cascade is described in reference 6. For this investigation there were 12 blades installed in the cascade. During the investigation there was flow through all of the blades. However, to minimize entrance and exit guide wall effects, only the channels corresponding to the center blades were used for determining the flow conditions.

Blading

The basic blading used in this investigation (fig. 2) is of constant cross section. The profile and flow path of the blading (fig. 3) are the same as that of the mean section

of the stator blading described in reference 7. The blading has a thick, curved-back profile and has a relatively large wedge angle at the trailing edge. The blading is 10.16 centimeters (4.00 in.) high and has a 5.74-centimeter (2.26-in.) chord and a 4.14-centimeter (1.63-in.) pitch. The trailing-edge thickness of the basic blading is 0.178 centimeter (0.070 in.), and the nominal downstream turning angle is about 67°. The flow angle at the inlet was 0° (see fig. 3).

Blades having round and square trailing-edge geometries and three different trailing-edge thicknesses were investigated. The trailing-edge thicknesses were 0.013 centimeter (0.005 in.; essentially sharp edged), 0.178 centimeter (0.070 in.), and 0.330 centimeter (0.130 in.).

The round and square trailing-edge bladings were formed by modifying the basic blading. In order to minimize the effect of differences in the upstream flow path, the flow path between the suction and pressure surfaces upstream of the trailing edge were the same for all blading. To achieve this, the suction- and pressure-side curvature and surface lengths of all bladings were kept the same as the basic blading. The profile thicknesses of the bladings were then adjusted to provide for the different trailing-edge thicknesses. Then the pitch of each blade configuration was adjusted to achieve the same flow path up to the trailing edge as that of the basic blading shown in figure 3 (excluding the leading-edge radius).

A cross sectional sketch of the profiles and flow paths of the blading with round trailing edges of different thicknesses installed in the cascade is presented in figure 4. As shown, three blades were modified. The center blades, which are the tested blades, have the same adjoining flow path except for leading-edge radii. Also, each tested (center) blade except the sharp-edged blade was adjacent to a blade of the same profile. As indicated, the sharp-edged blade was adjacent to blading with a 0.178-centimeter (0.070-in.) trailing-edge thickness. (This was done to simplify the manufacture and assembly of the sharp-edged blade set.) As will be explained in the section RESULTS AND DISCUSSION, the downstream flow conditions of the sharp-edged blading were affected by the adjacent blades with thicker trailing edges.

Instrumentation

The array of 155 wall-static-pressure taps, used for obtaining the flow conditions downstream of the blading, and the location of the taps relative to the blading is shown in figure 5. The distance between taps varied from about one-tenth to one-sixteenth of a blade pitch. As shown, the array covered essentially one blade pitch and extended, on the average, about 1.4 blade pitches downstream of the blading in the direction of flow. Mercury tube manometers were used to measure the pressures sensed by these taps.

Exit static pressures and flow angles were also measured downstream of the blading at two locations using a multipurpose survey probe of the type shown in figure 6. Details of the probe are described in reference 6. The three sensing elements are for measuring total pressure, static pressure, and flow angle. The total-pressure element, although used (as will be discussed later) was not essential to this particular investigation. Calibrated strain-gage transducers were used to measure the pressures sensed by the probe elements.

Test and Calculation Procedure

Atmospheric air was caused to flow through the cascade by use of the laboratory exhaust system. With atmospheric inlet conditions to the blading, desired pressure ratios across the blading for the desired critical velocity ratios $\left((V/V_{cr})_{i,m}\right)$ were set by adjusting an exhaust control valve. The range of critical velocity ratios investigated was from about 0.5 to 0.85. At the desired pressure ratio settings, photographs of the manometer tubes for the array of static-pressure taps were taken. In addition, using the calibrated probe, surveys of exit flow angle and exit static pressure were made at the blade mean section for approximately one blade pitch at two locations approximately 1/4 and 3/4 of a blade pitch downstream of the trailing-edge plane in the direction of flow.

Using the angle survey data, experimental values of flow angle reported in the results were determined from the angle probe calibration data. Using downstream static-pressure data obtained either from the static-pressure tap array or from surveys with the static-pressure probe, experimental values of isentropic kinetic energy ratio $\Delta H_{i,x}/\Delta H_{i,m}$ (see the SYMBOLS) were computed from the basic relation

$$\frac{\Delta H_{i,x}}{\Delta H_{i,m}} = \left[\frac{1 - \left(\frac{p_x}{p_0'}\right)^{(\gamma-1)/\gamma}}{1 - \left(\frac{p_m}{p_0'}\right)^{(\gamma-1)/\gamma}}\right]$$

The isentropic kinetic energy ratio corresponds to the pressure parameter $p_0' - p_x/p_0' - p_m$ for incompressible flow. The isentropic kinetic energy ratio was used for this investigation instead of the pressure ratio parameter because the pressure ratio parameter excludes compressibility effects.

Analytical values of flow angle and isentropic energy ratio reported in the results were obtained using the computer program described in reference 5.

RESULTS AND DISCUSSION

The results concern experimentally and analytically determined variations in flow conditions in the area around the exit and downstream of certain curved-back stator blading with thick profiles having round and square trailing edges of different thicknesses.

The experimental data were measured in a two-dimensional cascade. Flow-angle and exit-static-pressure data were obtained. Results are included for a range of ideal critical velocity ratios $(V/V_{cr})_{i,m}$ from about 0.5 to 0.85. Design $(V/V_{cr})_{i,m}$ for the basic blading is about 0.8.

The results are reported in terms of flow angles and isentropic kinetic energy ratios $(\Delta H_{i,x}/\Delta H_{i,m})$. The isentropic kinetic energy ratio is defined as the specific isentropic kinetic energy between total conditions at blade-row inlet and the static pressure at any given location in the blade row divided by the specific isentropic kinetic energy between total conditions at blade row inlet and the uniform static pressure downstream of the blade row.

Experimental results are presented and discussed first. Then the analytical results are presented and compared with experimental results.

Experimental Results

The experimentally determined variations in exit-flow conditions are presented in three parts. First, the effects of fluid flow velocity on exit-flow conditions for blading with fixed geometry are presented. Then, the effects on exit-flow conditions of blading with the same trailing-edge geometry but different trailing-edge thicknesses are compared. And last, the effects due to blading with round and square trailing edges of the same thickness are presented and compared.

Effect of fluid flow velocity on exit flow conditions for blading with fixed geometry. - Figure 7 presents contours of isentropic kinetic energy ratios around the exit and downstream of blading having a 0.178-centimeter (0.070-in.) thick square trailing edge for three different mixed-exit critical velocity ratios from 0.485 to 0.834. The contours of isentropic energy ratio also represent isobars of static pressure because the inlet conditions were constant. As indicated, the data used for determining these results were obtained from end-wall static-pressure taps.

The results show the isentropic energy ratio to vary from 0.7 to 1.20 in the measurement area. The patterns of energy ratio are similar for the three levels of velocity ratios, with the amplitude of variations increasing somewhat with increasing velocity level. The results also show that the energy variations are largely attenuated approximately one blade pitch downstream of the blading in the general direction of flow.

In figure 8, isentropic energy ratio variations are presented in a different manner to more clearly compare differences due to different overall fluid velocity levels through the stator blading.

Figure 8(a) shows the variation in energy ratio around the suction and pressure surfaces of the blading near blade exit and also downstream of the blading in plane A, which is the plane through the center of the trailing edge at a nominal flow angle of 65° (see fig. 7). The results in figure 8(a) show that the variations in energy ratio were not greatly affected by the fluid velocity level through the stator. The amplitudes of energy ratios in plane A (see fig. 7), beginning about 1/2 of a blade pitch downstream of the trailing edge increase moderately with increased fluid velocity level. However, the minimum energy ratios in plane A and the energy ratios at the trailing-edge surface are about constant for the range of fluid velocity levels investigated. At the maximum fluid velocity shown, the energy ratios in plane A vary from a minimum of about 0.8 to a maximum of about 1.05. Also, the lowest energy ratios occur roughly one-tenth of a blade pitch downstream of the trailing edge in the direction of flow, and the highest energy ratios occur about 1/2 to 2/3 of a blade pitch downstream of the trailing edge. Neglecting blade losses, low energy ratios imply low fluid velocities, and high energy ratios imply high fluid velocities. The variations in energy ratio in plane A will be considered more fully in the section Analytical Results and Comparison with Experimental Results.

In figure 8(b), the variation in isentropic energy ratio in the plane of the trailing edge is presented. The results for this plane show (as did those of fig. 8(a)) that the maximum amplitude of energy ratio increases moderately with increased critical velocity ratio, while the minimum amplitude of energy ratio remains essentially constant with increased velocity level. The gradients and amplitude of energy ratio are quite large. The maximum value of energy ratio varies from about 1.20 at the highest critical velocity ratio to about 1.10 at the lowest critical velocity ratio investigated, while the minimum value of energy ratio has a constant value of about 0.8. These large amplitudes and gradients in energy ratio in the trailing-edge plane, of course, imply large variations in velocity and static pressures. These variations, along with large flow-angle variations, are believed to be largely responsible for the errors in experimentally determined blade row loss that occur when the total-pressure probe sensing element is too close to the blade trailing edge and when average exit static pressures are assumed in the loss calculations (see refs. 1 and 2). These variations may also have a harmful effect on rotor blade row efficiency if the stator to rotor blade spacing is too small (see ref. 3).

In figure 9, a comparison of variations in flow angles at three different velocity ratios for the same blading as shown in figures 7 and 8 is presented. The results were measured by surveying 1.14 centimeters (0.45 in.) (roughly 1/4 blade pitch) downstream of the blading in the nominal direction of flow with the angle probe fixed at 65° from axial

at the blade mean section. The results show essentially identical trends in angle variation. The maximum flow angle variation in this plane was about $\pm 4^{\circ}$ and is considered quite large. The maximum angle difference, due to velocity ratio, is about 1°.

In summary, large variations in energy ratio and flow angle were found to exist in the trailing-edge plane and for at least 1/4 blade pitch downstream of the trailing edge in the direction of flow. The same trends in variations occurred for the relatively wide range of fluid velocities investigated. The maximum variation in amplitude of energy ratio did increase somewhat with increased fluid velocity level, but the minimum energy level remained constant with changing fluid velocity level. Similar trends and variations in flow conditions will be found for the blading with different trailing-edge thicknesses and trailing-edge geometries to be reported subsequently. However, the trends and variations will be shown to be somewhat affected by trailing-edge thickness and geometry.

It should be noted that the blading investigated was curved back with a relatively large wedge angle at the trailing-edge (see fig. 3). It would be expected that the variations in flow conditions reported for this blading would be reduced for blading having smaller wedge angles or less suction surface curvature downstream of the throat.

Effect of trailing-edge thickness on exit flow conditions for blading with round trailing edges. - Figure 10 compares contour plots of isentropic energy ratios around the exit of blading with round trailing edges of different thicknesses. The data shown was based on wall-static pressure tap measurements at a critical velocity ratio of approximately 0.85. The results in figure 10 are for trailing-edge thicknesses of 0.013 centimeter (0.005 in.; essentially sharp-edged), 0.178 centimeter (0.070 in.), and 0.330 centimeter (0.130 in.). It will be noted that in figures 10(b) and (c) the results were extrapolated (dashed portions of the curves) outside the measuring area to include two blades, but in figure 10(a) the results were not extrapolated outside the measuring area. The reason for this difference was caused by the following.

As discussed previously in the section APPARATUS AND PROCEDURE and as shown for the blading of figures 10(b) and (c), each test blade was adjacent to two blades having the same profile. As a result, for these bladings the measured isobars on the suction side of the blading matched well with those on the pressure side when displaced one blade pitch. Thus, it was indicated that the contours of energy ratio for the adjacent blades were the same as for the tested blade. However, the sharp-edged test blade shown in figure 10(a) was not adjacent to blades with the same profile, the adjacent blades having thicker trailing edges. As a result, the measured isobars on the suction side of the test blade did not quite match those on the pressure side of the adjacent blades when displaced one blade pitch. This indicated that the adjacent dissimilar blades affected the energy ratio contours of the test blade to some extent, even though the flow path adjacent to all tested blading up to the trailing edge were the same for all sets of blading. This discrepancy in the results shown in figure 10(a) was apparently caused by the fact that the

adjacent blading, as a result of the thicker trailing edges, had different surface pressure distributions than the test blade. These different pressures were reflected into the flow path of the test blade. Thus, the results for the sharp-edged blade (fig. 10(a)) must be considered in error, to some degree, relative to results that would have been obtained had the adjacent blades been the same as the tested blade.

In general, the results in figure 10 indicate an increase in amplitude and gradient of isentropic energy ratio with increased trailing-edge thickness, with the variations in energy ratio being largely attenuated at a distance of about one blade pitch downstream of the trailing edge plane in the direction of flow. Differences due to trailing-edge thickness are shown more clearly in the following results.

Figure 11 compares the variations in isentropic energy ratio for the blading with different round trailing-edge thicknesses along the suction and pressure surfaces near blade exit and in two different planes downstream of the blading.

Figure 11(a) compares the variations around the suction and pressure surfaces of the blading near blade exit and downstream of the blading in plane A (defined in fig. 10). These results confirm the general increase in amplitude of variation in isentropic energy ratio with increased trailing-edge thickness (fig. 10). At the intersection of plane A and the trailing edge, the increase in energy ratio with increasing trailing-edge thickness indicates a reduction in static pressure with increased trailing-edge thickness. Reduced static pressures and increased trailing-edge thickness, of course, imply increased blade row loss due to increased base drag. This indicated trend of increasing blade loss with increased trailing-edge thickness is confirmed in reference 4, which reports the trailing-edge loss quantitatively for these bladings.

Figure 11(b) compares the isentropic energy ratio in the trailing-edge plane (plane B, fig. 10) for the blading with round trailing edges of different thicknesses. The results for this plane also indicate some increase in amplitude of energy ratio with increased trailing-edge thickness. The largest difference in amplitude for the blade with the thickest trailing edge is from a maximum value of 1.20 to a minimum of about 0.8. The total variation in energy ratio of about 40 percent is considered large.

Figures 12 and 13 present comparisons of isentropic energy ratios as determined from wall static-pressure-tap measurements with energy ratios determined by survey measurements at the blade mean section with a calibrated static-pressure probe. Figure 12 shows the comparison for the three round trailing-edge bladings of different thickness for plane C (fig. 10). This plane is 1.14 centimeters (0.45 in.), or roughly 1/4 blade pitch, downstream of the trailing-edge plane in the general direction of flow. Figure 13 shows the same comparison for two round trailing-edge bladings of different thicknesses in plane D. This plane is 2.92 centimeters (1.15 in.), or roughly 3/4 blade pitch, downstream of the trailing edge in the direction of flow. The results in the two figures show excellent agreement in trends and fair agreement in magnitude. The results indicate that for most of the cases the average energy level as determined by either

measurement method is about the same.

Comparing figures 12 and 13 shows that the energy ratio variation attenuates fairly rapidly in the direction of flow. The change in amplitude of energy ratio in plane C varies from a maximum value of about 1.20 to a minimum of about 0.75. In plane D, the change in amplitude of energy ratio is reduced to a maximum value of about 1.05 and a minimum value of about 0.90. This is a reduction in amplitude variation from about 0.45 to 0.15 in a distance of 1/2 blade pitch in the direction of flow. As previously mentioned, the variations in energy ratio are largely attenuated at a distance of approximately one blade pitch downstream of the blading in the direction of flow.

It was also desired to establish the approximate location of the blading relative to the maximum and minimum values of energy ratio as determined by the two methods of measurement. The location of the blading relative to the energy ratios is indicated in figures 12 and 13 by the wake points. In figures 12 and 13, for the wall tap measurements, the location of the wake peak (the point of maximum total pressure loss in the wake) was assumed to be at the intersections of planes A and C, and A and D, respectively, as shown in figure 10. For the probe measurements, the location of the wake point corresponds to the peak value of wake pressure loss relative to the isentropic energy ratios as determined from simultaneous x-y traces of pressure loss and downstream static pressure. The location of the peak of the wake trace relative to the exact location of the blading is, of course, affected by variations in flow angle between the trailing-edge plane and the downstream plane in question. The small differences in indicated location of the blading relative to the energy ratios may therefore be due to the assumption of constant 65° flow angle used in determining the location of the blading for the pressure-tap results. Also the results for the wall tap data were obtained with the static pressure probe removed from the flow path; whereas, all the results obtained from probe data were obtained with the probe in the flow path. Since the probe itself distorts the flow (ref. 1), the discrepancy in results in figures 12 and 13 may also be partly due to probe blockage.

In figure 14, a comparison is shown of flow angles, measured at the mean section for the three bladings with different round trailing-edge thicknesses. The flow angles are compared in plane C (see fig. 10) in figure 14(a) and in plane D (see fig. 10) in figure 14(b).

The results in figure 14(a), for plane C, which is roughly 1/4 blade pitch from the trailing-edge in the direction of the flow, shows an increase in flow angle gradient with increased trailing-edge thickness. The amplitude of the flow angles for the two bladings with the thicker trailing edges are about the same and are larger than the amplitude of the blading with the sharp trailing edge. However, as previously noted, the results for the sharp-edged blade may have been somewhat affected by the thicker trailing edges of the adjacent blading.

In figure 14(b), the angle results for plane D, measured roughly 3/4 of a blade pitch from the trailing-edge in the direction of flow, indicate that the amplitude and variation in flow angle for the three bladings are about the same. The amplitude of flow angle variations for the blading with thicker trailing edges shown in plane C nearer the trailing edge must therefore attenuate more rapidly than for blading with thinner trailing edges.

Comparing the results in figures 14(a) and (b) shows that all the flow angle variations attenuate fairly rapidly in the direction of flow. The largest amplitude of flow angle variation is about $\pm 4.5^{\circ}$ in plane C. This change in amplitude of flow angle is considered fairly large. In plane D, the amplitude of flow angle variations are reduced to less than about $\pm 2^{\circ}$. Although flow angle measurements were not made further downstream, these results indicate that the angle variations are largely attenuated, as were the energy ratio variations, at a distance of about one blade pitch downstream of the trailing edge in the direction of flow.

References 1 and 2 report that overall blade-row losses based on total-pressure survey loss measurements which were taken too close to the trailing edge (about 1/10 of a blade pitch or less) may be in error if average values of exit-flow angles and average values of exit static pressures obtained from end-wall taps are used in computing the overall loss. The evidence in these references, as well as in the subject report, indicates that this error is caused by large variations in the amplitude and gradients of flow angle and static pressure very near the trailing edge. It is believed that these large variations cannot be defined accurately by the survey probe employed because the physical dimensions of the probe sensing elements are too large.

Also, as reported in references 1 and 2, it was found that consistent overall blade row losses could be obtained if the total-pressure loss measurements were made at greater distances, roughly 1/4 to 1 blade pitch downstream of the blading in the direction of flow, using average values of flow angles from survey measurements and average values of static pressures from wall static-pressure tap measurements.

Considering the relatively large variations in static pressures and flow angles indicated in figures 12 to 14, even at these larger distances downstream of the blading, it is not apparent why close agreement in values of blade row losses can be obtained using average values of flow angle and static pressure. Therefore, computations were made of blade row losses based on data at two downstream locations (planes C and D) using both variable values of flow angle and static pressure (as determined by the multipurpose survey probe) and also using average values of flow angle and static pressure. The difference in overall blade row efficiency loss based on variable and constant exit conditions was less than 0.1 of a percent.

The reason for the close agreement in results for the two examples computes is this: In the loss region (i.e., in the wake of the blading), when using variable exit conditions, the effects of variable flow angle and variable exit static pressure are compensating so that the same loss in kinetic energy is obtained as when using average exit

conditions. It should be cautioned, however, that, although average downstream conditions (determined as described in ref. 1) could be used to compute correct blade row losses for this particular stator blading, this method may not apply for all blading. It is therefore recommended that static-pressure, total-pressure, and flow-angle data for the computation of blade row losses be determined from survey measurements at least 1/2 blade pitch downstream of the trailing edge in the direction of flow using a calibrated multipurpose probe and that the blade row loss then be computed by integration of the varying flow conditions over the blade row passage. This recommendation applies particularly for blading with large wedge angles at the trailing edge (see fig. 3) or large trailing-edge thicknesses.

Effect of round and square trailing-edge geometry on exit flow conditions for blading with trailing-edge thickness of 0.330 centimeter (0.130 in.). - A comparison of isentropic energy ratios and flow angles for the round and the square trailing-edge geometry blades is presented in figures 15 to 17. Figure 15 compares contours of isentropic energy ratios; figure 16 compares isentropic energy ratios in four selected planes; and figure 17 compares the flow angles in two selected planes.

The comparisons for the two blades on the three figures show that the contours and the trends and amplitudes of the variations in energy ratio and flow angle are generally the same. Some small differences do exist. With one important exception, these differences are believed to have no significant effect on the performance of the two blades. The important exception is the difference in energy ratio at the trailing edge (fig. 16(a)). Here, the energy ratios between points W and X for the blading with square trailing edges, although about the same width, are somewhat higher than the energy ratio between points Y and Z for the blading with round trailing edges. As previously discussed, a higher energy ratio of the same width at the trailing edge implies a lower pressure over the same area at the trailing edge, and, consequently, a larger trailing-edge loss. The larger loss indicated here for the blading with square trailing edges is confirmed quantitatively in reference 4.

Analytical Results and Comparison with Experimental Results

These results concern certain turbine stator blading with round trailing edges of three different thicknesses. The thicknesses are 0.013 centimeter (0.005 in.; sharp-edged), 0.178 centimeter (0.070 in.), and 0.330 centimeter (0.130 in.). The analytical results were obtained from the program of reference 5, which was written for blading with sharp and round trailing edges only. The experimental results were obtained as previously described under APPARATUS AND PROCEDURE. Where comparative performance is shown, the experimental contour plots are the same as those previously

presented under Experimental Results. Variations in isentropic energy ratio and flow angle near the exit and downstream of the blading are reported.

Figures 18, which is in three parts, reports and compares analytically and experimentally determined contours of isentropic energy ratio for bladings with the three different trailing-edge thicknesses. It will be noted that many of the comparisons shown are for nearly the same values of $(V/V_{cr})_{i,m}$, while other comparisons are at somewhat different values of $(V/V_{cr})_{i,m}$. The largest difference in critical velocity ratio for any comparison is 0.70 to 0.85, which is for one case only. However, with figures 7 to 9 for blading of fixed geometry, the trends and amplitudes of flow angle and energy ratio were about the same over a fairly wide range of fluid velocity levels with the exception that the maximum amplitude of energy ratio increased moderately with increased fluid velocity level. It is therefore the opinion of this author that the comparisons between experimental and analytical results for the same blading are not seriously affected by these moderate differences in velocity levels.

For figures 18(b) and (c), the analytical contours of energy ratio include some interpolation in the trailing-edge region represented by the dashed contours. This is because the analytical results are based on ideal theoretical flow, which requires that the pressure at the trailing-edge stagnation point be equal to inlet total pressure. To perform the interpolation, the solid isobars were first plotted and then connected by the dashed isobars.

The results in figure 18 indicate patterns of energy ratios for the experimental and analytical results, which are generally similar. However, the analytical contours of isentropic energy ratio are more closely spaced than the experimental contours, particularly near the trailing edge. Thus, it is indicated that the analytically determined gradients in isentropic energy ratio are greater than the experimental gradients. This fact will be shown more clearly on the following figures.

In figure 19, a comparison is presented of experimentally and analytically determined isentropic energy ratios along the suction and pressure surface of the blading near the blade exit and also in plane A (see fig. 18) through the center of the trailing edge at a nominal flow angle of 65° from axial.

As indicated by figure 18, figure 19 shows the analytically determined gradients in energy ratio to be steeper than the experimentally determined gradients, particularly near the trailing-edge. The amplitude of the analytical variations are also larger than the experimental, but the trends of analytical and experimental results are quite similar.

In figure 19, the comparison of experimental with analytical results at the intersection of plane A with the trailing edge for the three different bladings shows good agreement in the energy ratios for the blading with thin trailing edges (fig. 19(a)), rather poor agreement for the blading with 0.178-centimeter (0.070-in.) trailing-edge thickness (fig. 19(b)), and excellent agreement for the blading with 0.330-centimeter (0.130-in.) trailing-edge thickness (fig. 19(c)).

The minimum value of energy ratio just downstream at the trailing-edge is less for the analytical results than for the experimental, with the difference between the minimum values of analytical and experimental values increasing with increasing trailing-edge thickness. Several possible reasons exist for these differences. Included among these are the following. The analytical results are for infinite span blading with unobstructed downstream flow, so there are no end-wall or side-wall effects. The analytical results also assume ideal flow with no losses. The analytical results can also be significantly affected by the value of uniform downstream flow angle assumed as an input value for the analytical method. However, the fact that the analytical value of energy ratio converge at the intersection of plane A with the trailing edge (see fig. 19) indicates that the correct downstream angle was chosen.

On the other hand, the experimental results are for a finite cascade. Therefore, contrary to the analytical results, any side-wall effects and end-wall effects present are included in the experimental results as are all effects of losses caused by the flow of a real fluid.

In figure 20, experimentally and analytically obtained values of isentropic energy ratio for the bladings with different trailing-thicknesses are compared in the trailing-edge plane. The trends of experimental and analytical results agree quite well; however, the amplitudes and gradients of the analytical variations are larger than the experimental.

Figures 21 and 22 compare experimental and analytical values of isentropic energy ratio for the bladings with different trailing-edge thicknesses in two planes at different distances downstream of the trailing edge. (It should be noted that the data used for obtaining the experimental results were obtained with the static-pressure survey probe.)

Figure 21 compares the results in plane C (see fig. 18), roughly 1/4 of a blade pitch downstream of the trailing-edge plane in the direction of flow. And figure 22 compares the results in plane D, roughly 3/4 of a blade pitch downstream of the trailing-edge in the direction of flow. The agreement shown between experimental and analytical results in these two planes is considered to be generally good. The largest disagreement between experimental and analytical results is for the sharp-edged blading (figs. 21(a) and 22(a)). This larger disagreement for the sharp-edged blading probably occurs because the experimental results for the blading with sharp-trailing edge were affected by having adjacent blades with thicker trailing edges.

Figures 21 and 22 also show comparative locations of the blade wakes for the experimental and analytical results. This was done, as previously discussed under Experimental Results, in an effort to locate the position of the blading relative to the maximum and minimum values of energy ratio. The location of the wake point for the analytical results may be in error for the same reason that the experimental results determined from wall static-pressure-tap data may be in error; that is, the wake location was obtained by assuming that the flow angle between the trailing-edge plane and downstream

planes shown in the figures was a constant 65°, whereas the actual flow angle between the two planes, which is accounted for in results obtained using the survey probe, is variable. Also, probe blockage, as well as side-wall and end-wall effects, may have influenced the experimental results shown in figures 21 and 22.

Figures 23 and 24 compare experimental and analytical values of variations in average flow angle for the bladings with three different trailing-edge thicknesses. The results are for the same two downstream planes as shown in figures 21 and 22.

Figures 23 and 24 show that the trends and amplitudes of variations in experimental and analytical flow angles agree quite well, considering the possible reasons (previously given) for differences to exist. The largest difference between the experimental and analytical results is that shown in figure 24(a) for the sharp-edged blade in plane D. This difference may result from the aforementioned fact that in the experimental investigation the tested sharp-edged blade had adjacent blading with thicker trailing edges. The adjacent blading, then, had different surface pressures than the sharp-edged blading. These different surface pressures were reflected into the flow path of the sharp-edged test blade, causing the flow conditions, including the flow angles, of the sharp-edged blade to be affected.

The results of this section may be summarized as follows. Considering the fact that the analytical results are for an ideal fluid with no losses, whereas the experimental results are for a real fluid with actual losses, and also considering the other reasons previously discussed for differences in the results, the agreement between the results is considered generally fair to excellent.

SUMMARY OF RESULTS

The results concern experimentally and analytically determined variations in flow conditions in the area around the exit and downstream of certain curved back stator blading with thick profiles having round and square trailing edges of different thicknesses. The variations in flow conditions are reported in terms of isentropic energy ratio and flow angle.

The experimental data were obtained in a simple two-dimensional cascade. Analytical results were obtained by the program of reference 5. The range of average downstream fluid velocities investigated varied from an ideal mixed critical velocity ratio $(V/V_{cr})_{i,m}$ of about 0.5 to about 0.85.

The results are as follows:

1. Large variations in flow conditions exist in the trailing-edge plane and for a distance of at least a quarter of a blade pitch downstream of the blading in the direction of flow for all the blading tested and for all fluid velocities tested. For instance, in the

plane of the trailing edge, values of isentropic energy ratio varied as much as about ±20 percent across the blade pitch. Flow angles varied as much as about $\pm 4.5^{\circ}$ in a plane parallel to the trailing edge roughly 1/4 of a blade pitch downstream of the trailing edge in the direction of flow.

2. The flow variations attenuate fairly rapidly in the direction of flow. At a distance of about one blade pitch downstream of the trailing-edge plane in the direction of flow, the measured variations in energy ratio were essentially uniform.

3. For blading with the same trailing-edge geometry and critical velocity ratio, the static pressure at the trailing edge decreases significantly with increasing trailing-edge thickness, as evidenced by the increase in energy ratio. Decreased static pressure at the trailing edge implies increasing blade row loss with increasing trailing-edge thickness. The increased loss with trailing-edge thickness is confirmed quantitatively in the NASA publication TN D-6637.

4. For a particular blading, the same trends of flow variations occurred over the range of critical velocity ratios investigated. The maximum amplitude of energy ratio did increase somewhat with increased fluid velocity level, but the minimum value of energy ratio and the energy ratio at the trailing-edge surface were constant with changing fluid velocity.

5. For blading with round and square trailing-edge geometry having the same trailing-edge thickness of 0.330 centimeter (0.130 in.), the amplitude and trends of variation in energy ratio in the trailing-edge plane were about the same. However, the average static pressure at the trailing edge was somewhat lower for the square trailing-edge blade than for the round as implied by the higher energy ratio at the trailing edge of the square trailing-edge blade. This evidence indicates that the blading with square trailing edges has more trailing-edge loss than the blading with round trailing edges. This larger loss for square trailing-edge blading is confirmed quantitatively in the NASA publication TN D-6637.

6. A comparison was made between experimental and analytical results for three bladings having round trailing edges of significantly different trailing-edge thicknesses. The agreement between the results is considered to be fair to excellent considering the fact that the analytical results are for an ideal fluid with no losses, whereas the experimental results are for a real fluid with actual losses of the blade row.

Lewis Research Center,
National Aeronautics and Space Administration,
Cleveland, Ohio, August 2, 1972,
764-74.

REFERENCES

1. Moffitt, Thomas P.; Prust, Herman W., Jr.; and Schum, Harold J.: Some Measurement Problems Encountered When Determining the Performance of Certain Turbine Stator Blades From Total Pressure Surveys. Paper 69-GT-103 ASME, Mar. 1969.

2. Prust, Herman W., Jr.; Moffitt, Thomas P.; and Bider, Bernard: Effect of Variable Stator Area on Performance of a Single-Stage Turbine Suitable for Air Cooling. 5: Stator Detailed Losses With 70-Percent Design Area. NASA TM X-1696, 1968.

3. Schum, Harold J.; Szanca, Edward M.; and Behning, Frank P.: Effect of Stator-Rotor Axial Clearance on Cold-Air Performance of a Turbine With Transpiration-Cooled Stator Blading. NASA TM X-67914, 1971.

4. Prust, Herman W., Jr.; and Helon, Ronald M.: Effect of Trailing-Edge Geometry and Thickness on the Performance of Certain Turbine Stator Blading. NASA TN D-6637, 1972.

5. Katsanis, Theodore: Fortran Program for Calculating Transonic Velocities on a Blade-to-Blade Stream Surface of a Turbomachine. NASA TN D-5427, 1969.

6. Stabe, Roy G.: Design and Two-Dimensional Cascade Test of Turbine Stator Blade With Ratio of Axial Chord to Spacing of 0.5. NASA TM X-1991, 1970.

7. Whitney, Warren J.; Szanca, Edward M.; Moffitt, Thomas P.; and Monroe, Daniel E.: Cold-Air Investigation of a Turbine for High-Temperature-Engine Application. I - Turbine Design and Overall Stator Performance. NASA TN D-3751, 1967.

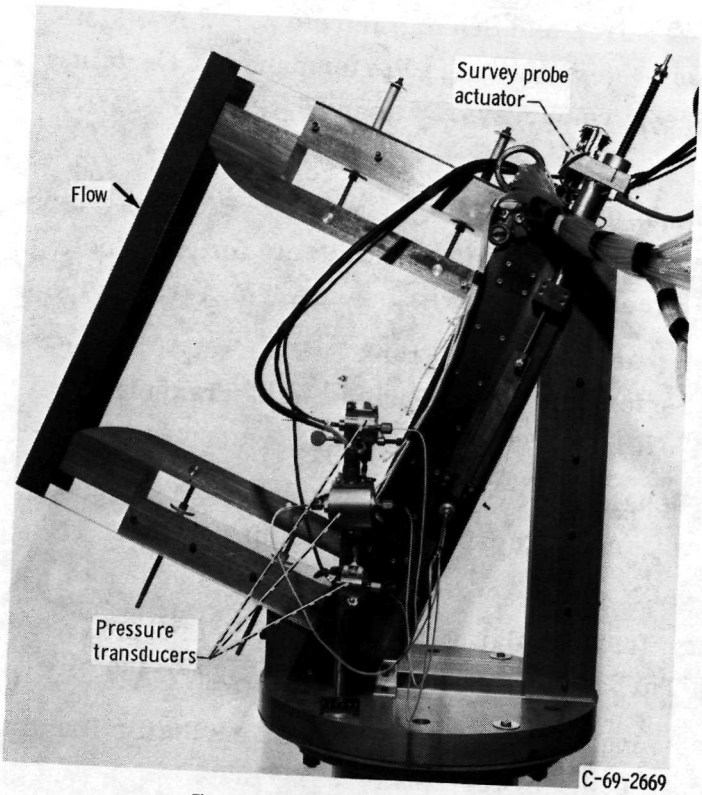

Figure 1. - Stator blade cascade.

Figure 2. - Basic stator blading.

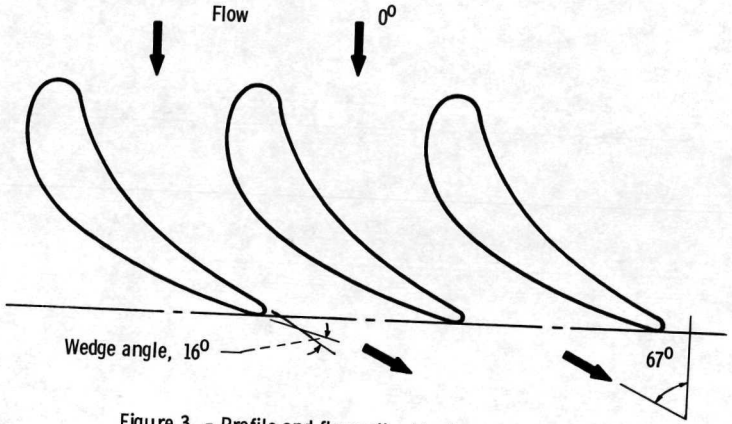

Figure 3. - Profile and flow path of basic stator blading.

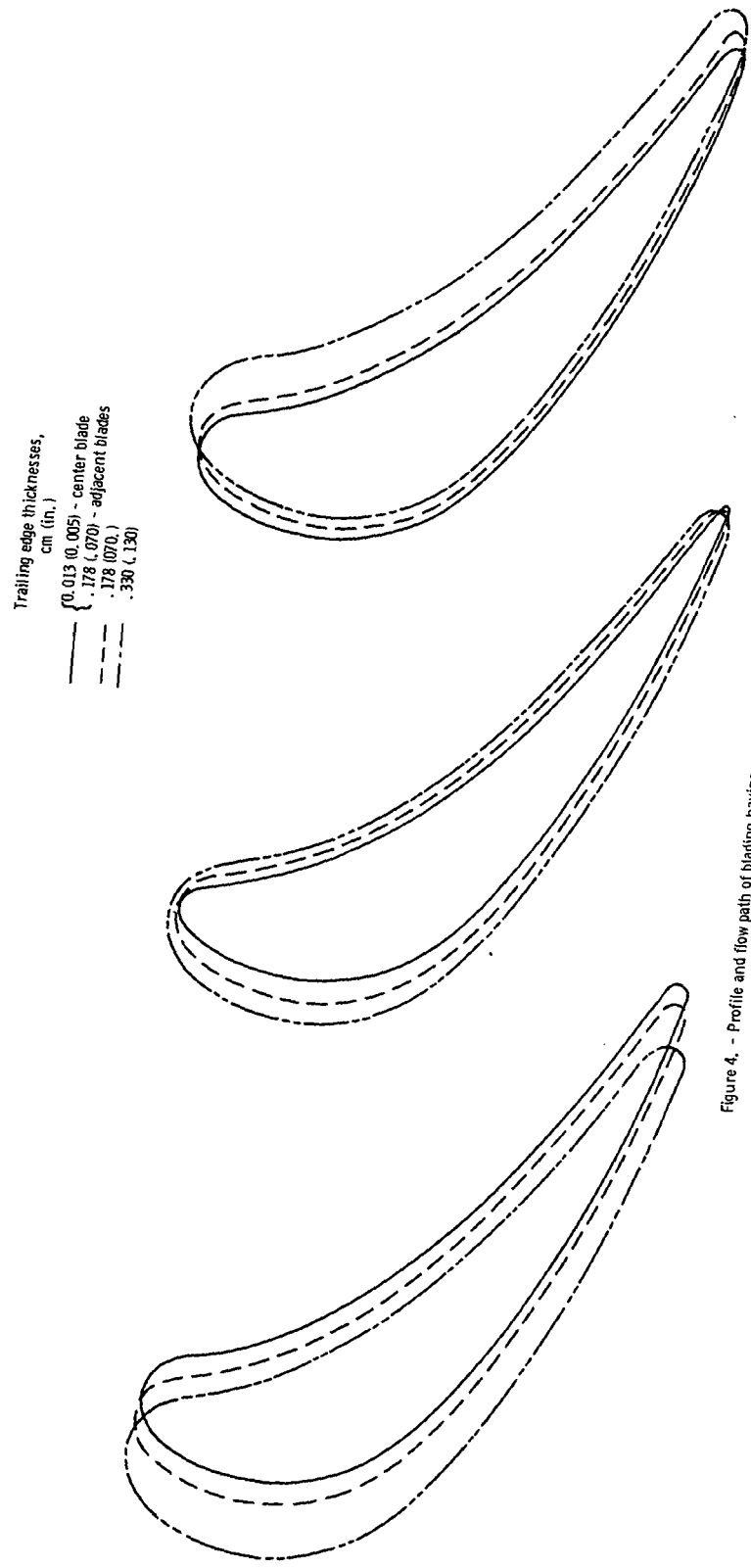

Figure 4. - Profile and flow path of blading having round trailing-edges of different thicknesses.

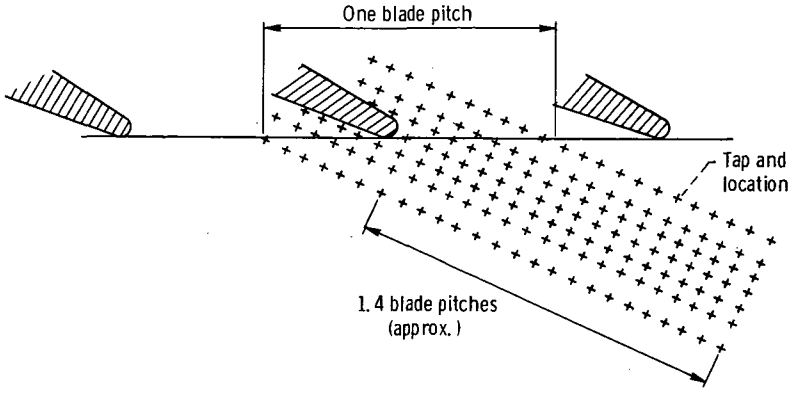

Figure 5. - Cross-sectional sketch of location of end-wall static-pressure taps relative to blading.

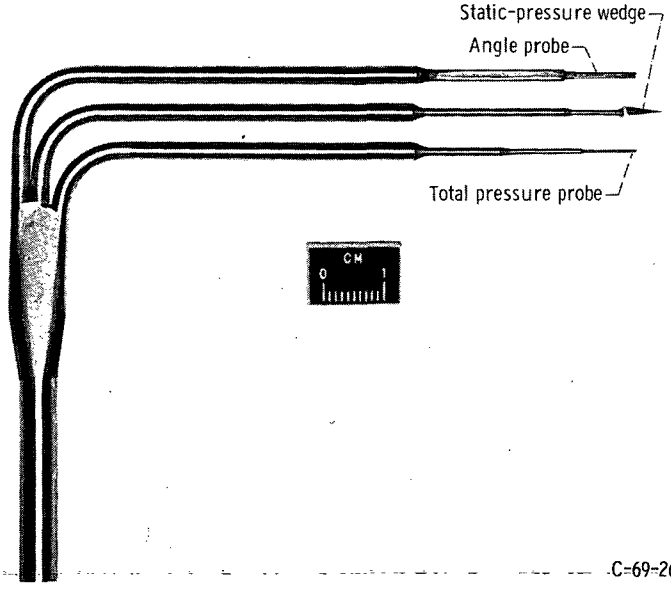

Figure 6. - Multipurpose survey probe.

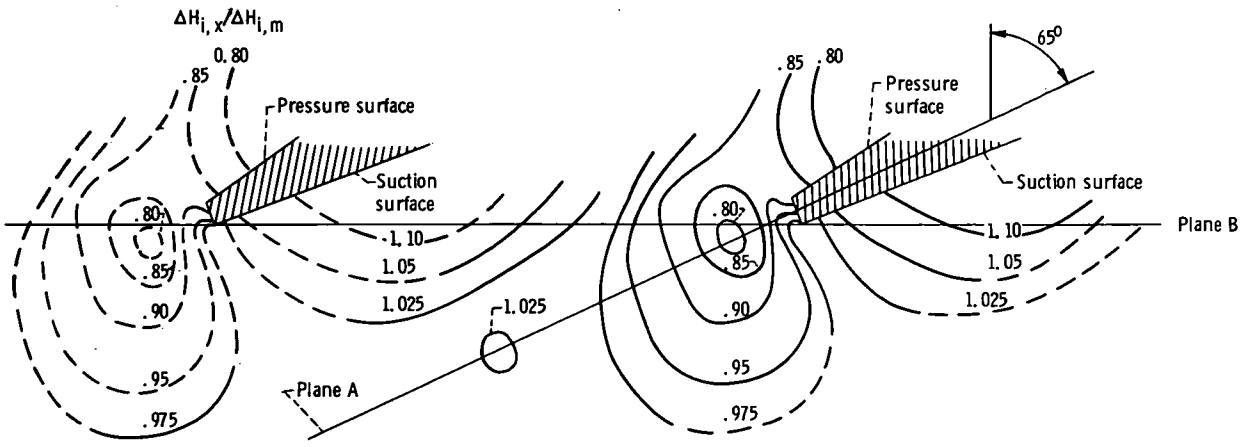

(a) Critical velocity ratio, 0.485.

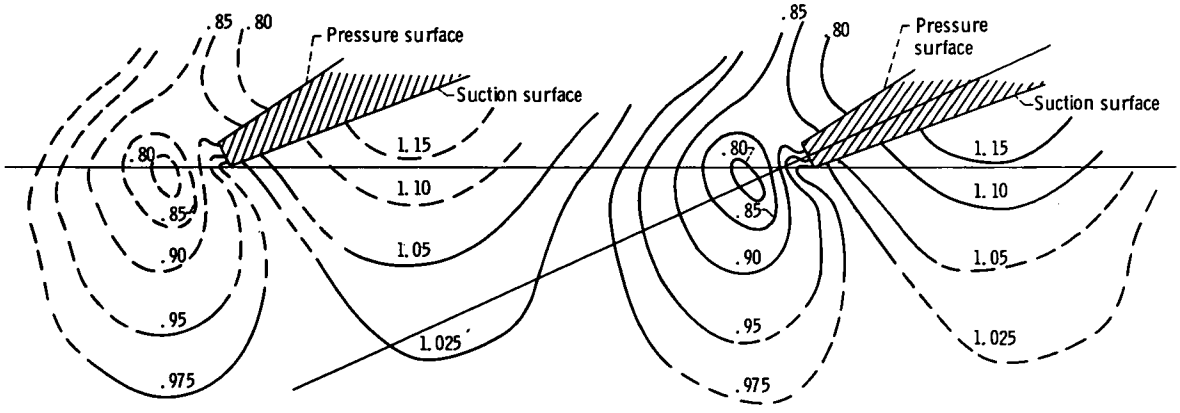

(b) Critical velocity ratio, 0.670.

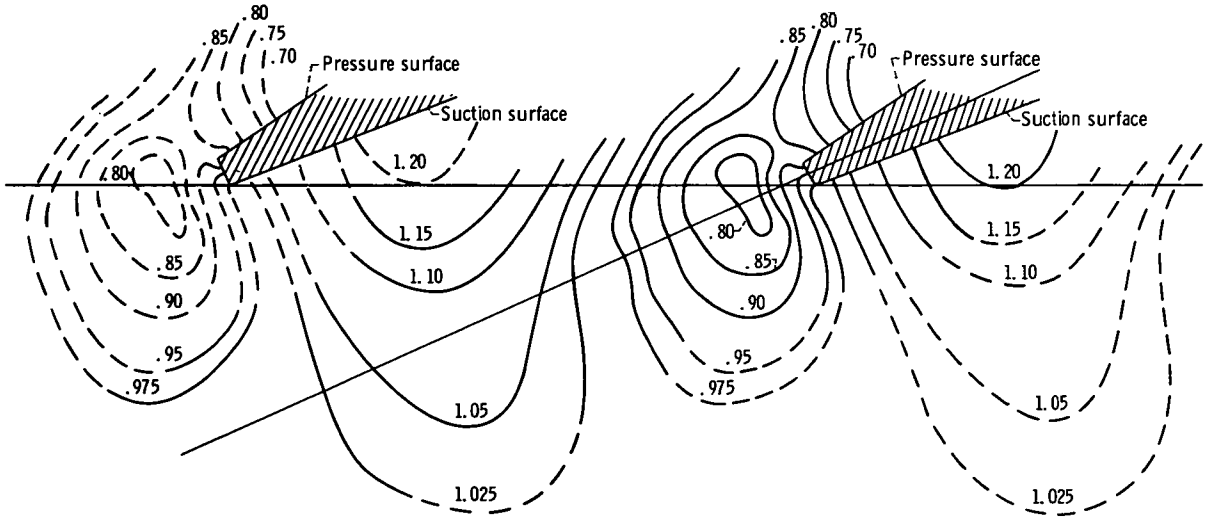

(c) Critical velocity ratio, 0.834.

Figure 7. - Contours of isentropic energy ratios $\Delta H_{i,x}/\Delta H_{i,m}$ for 0.178-centimeter (0.070-in.) square trailing-edge blade for different critical velocity ratios. Data measured by wall static-pressure taps.

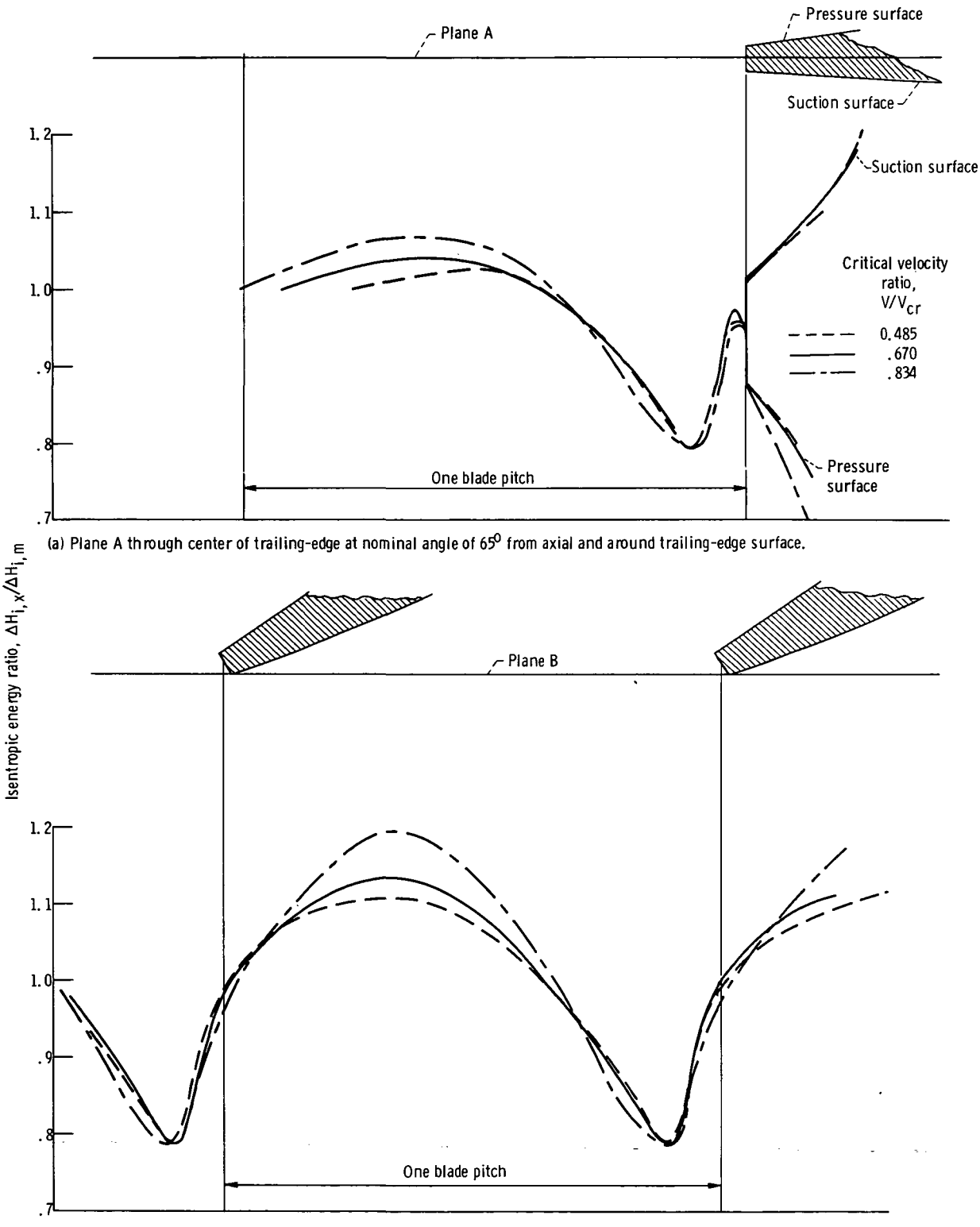

(a) Plane A through center of trailing-edge at nominal angle of 65^{0} from axial and around trailing-edge surface.

(b) Trailing-edge plane; plane B.

Figure 8. - Comparison of isentropic energy ratios for 0.178-centimeter (0.070-in.) square trailing-edge blade for different critical velocity ratios in two different planes and around trailing-edge surface.

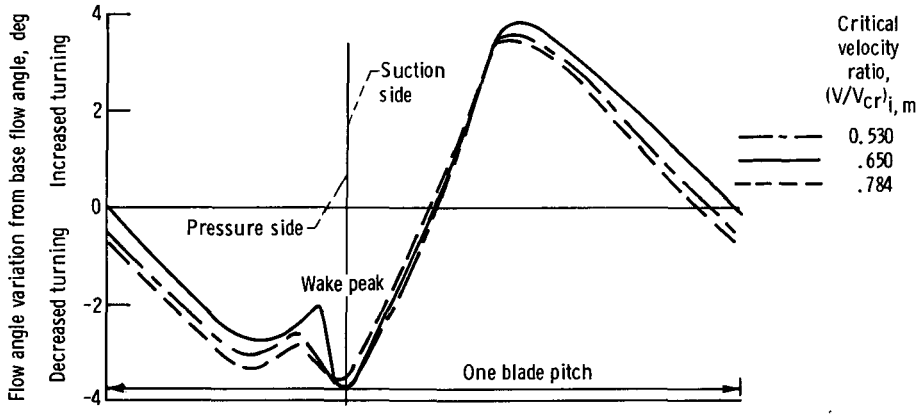

Figure 9. - Comparison of experimentally determined flow angles at different critical velocity ratios. Data for 0.178-centimeter (0.070-in.) square trailing edge, measured 1.14 centimeters (0.45 in.) downstream of blading at nominal angle of 65^0 from axial at blade mean section.

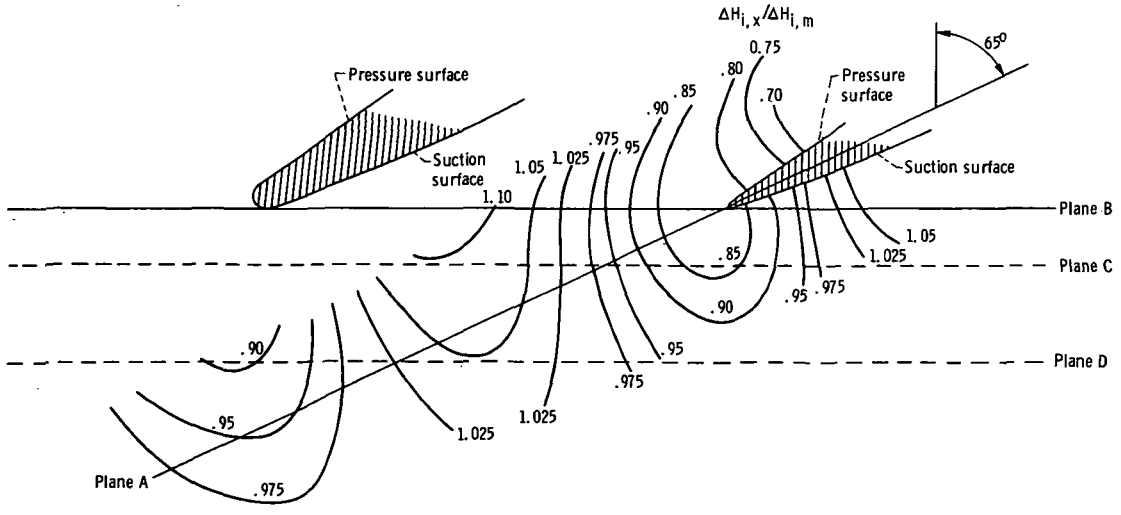

(a) Trailing-edge thickness, 0.013 centimeter (0.005 in.).

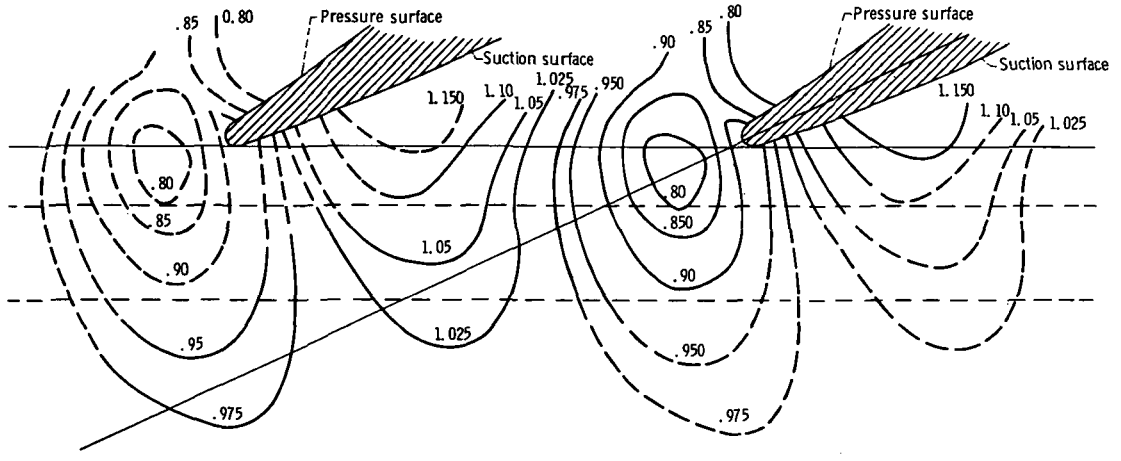

(b) Trailing-edge thickness, 0.178 centimeter (0.070 in.).

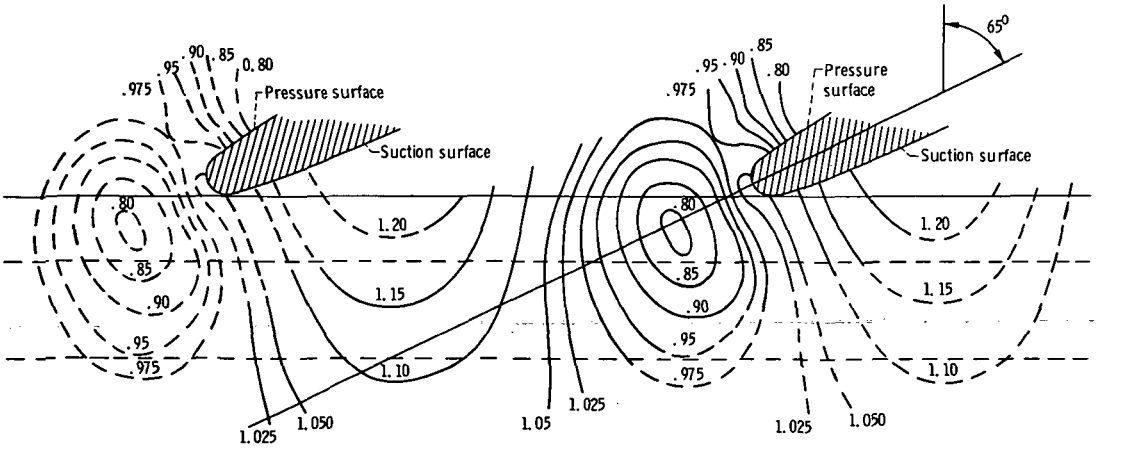

(c) Trailing-edge thickness, 0.330 centimeter (0.130 in.).

Figure 10. - Contours of isentropic energy ratios $\Delta H_{i,x}/\Delta H_{i,m}$ for blading with different round trailing-edge thicknesses. Critical velocity ratio, 0.85 (approx.). Data measured by wall static-pressure taps.

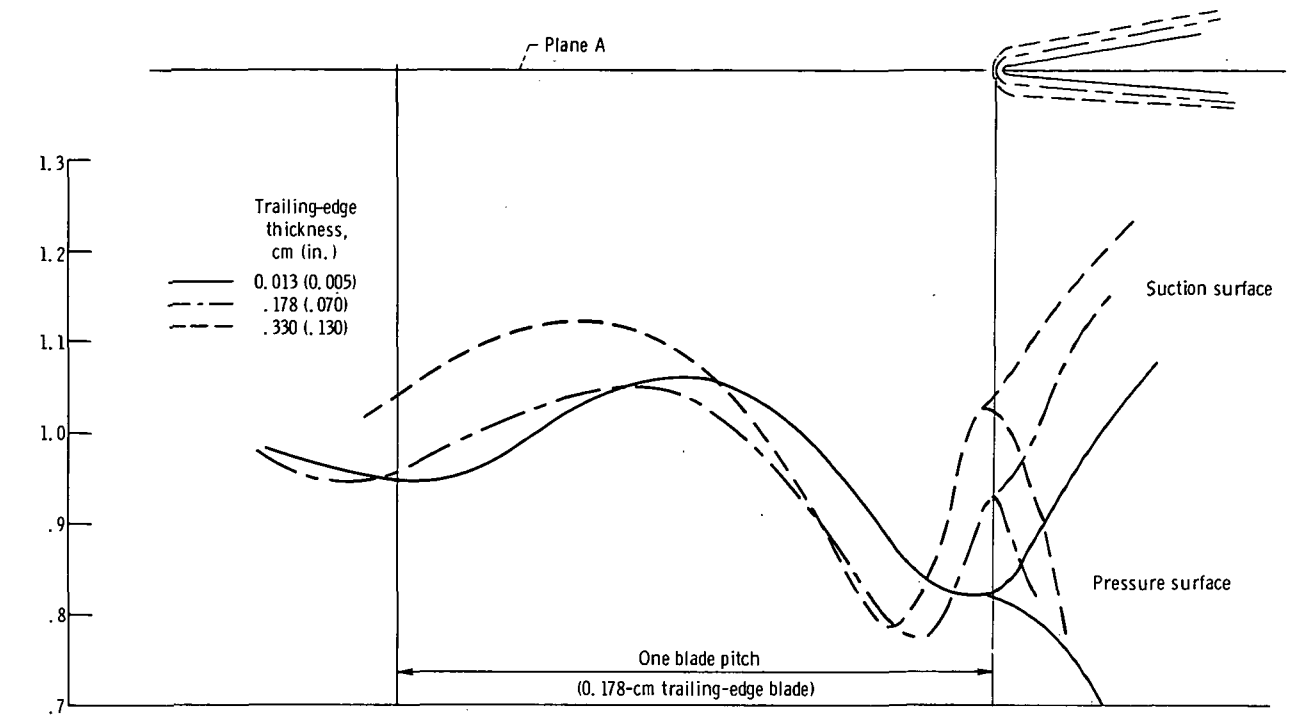

(a) Plane A through center of trailing edge at nominal angle of 65^0 from axial and around trailing-edge surface.

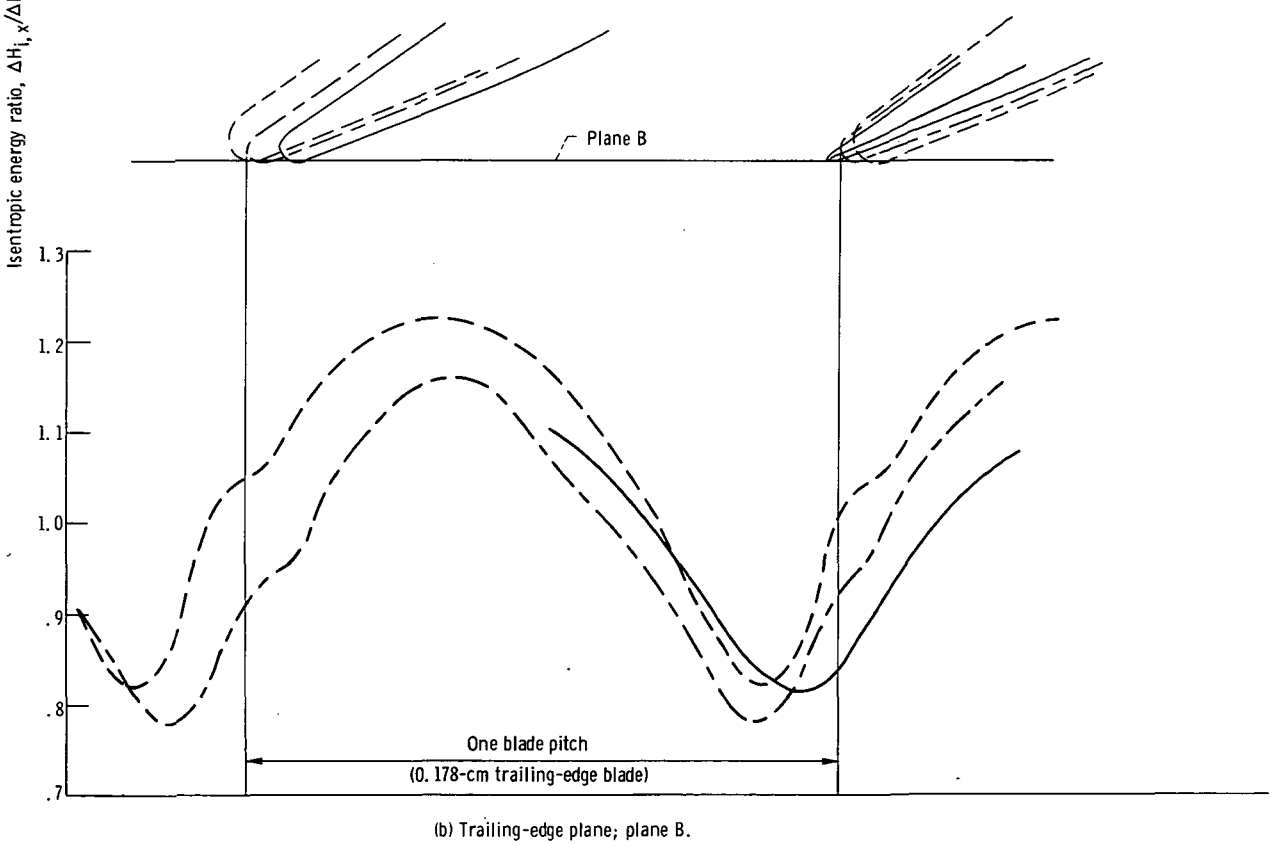

(b) Trailing-edge plane; plane B.

Figure 11. - Comparison of isentropic energy ratios for blading with different round trailing-edge thicknesses in two different planes and around trailing-edge surface. Critical velocity ratio, 0.85 (approx.).

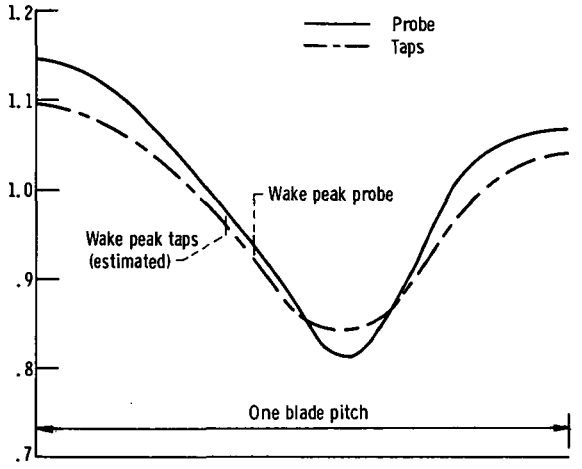

(a) Round trailing-edge thickness, 0.013 centimeter (0.005 in.).

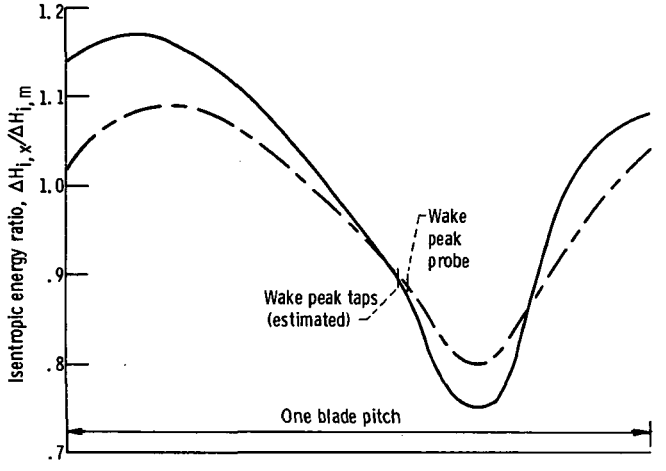

(b) Round trailing-edge thickness, 0.178 centimeter (0.070 in.).

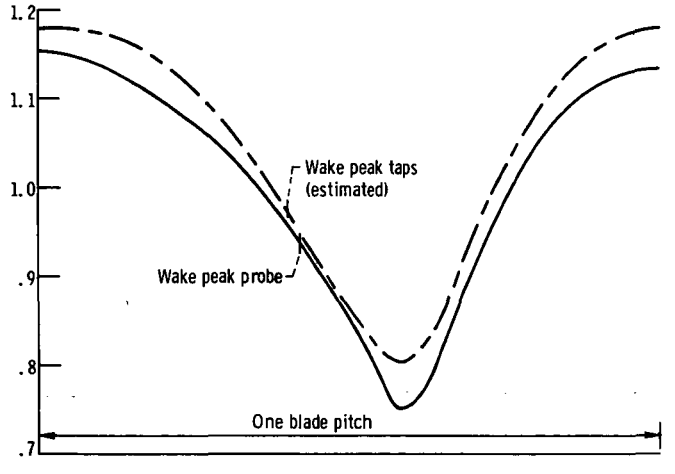

(c) Round trailing-edge thickness, 0.330 centimeter (0.130 in.).

Figure 12. - Comparison of isentropic energy ratios using data measured by static-pressure probe at blade mean section and by end-wall static-pressure taps. Data measured 1.14 centimeters (0.45 in.) downstream of blading at nominal flow angle of 65^{0} from axial, plane C (fig. 10); critical velocity ratio, 0.85 (approx.).

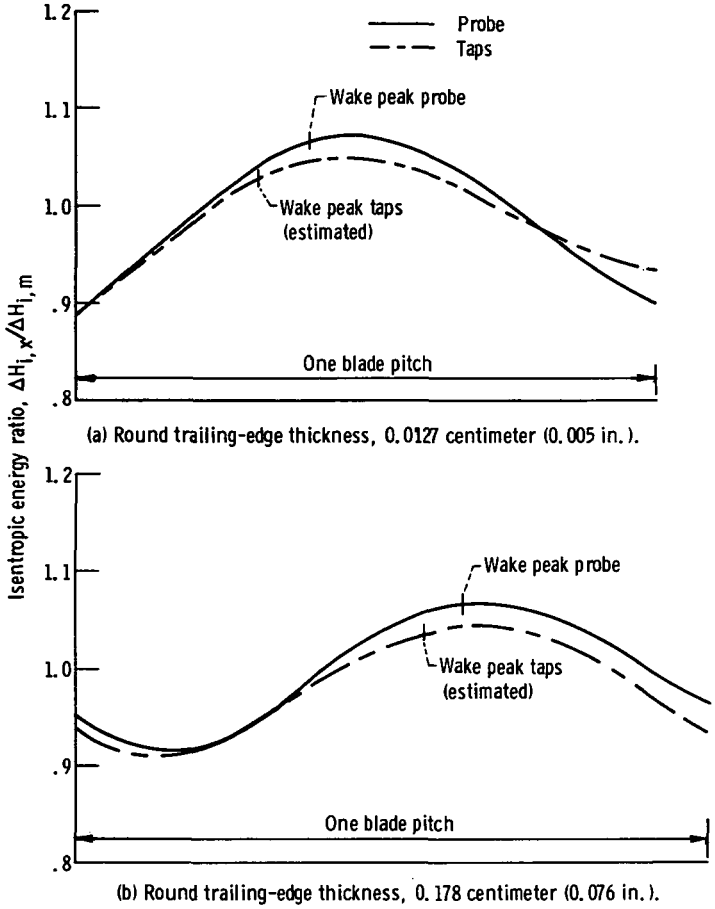

Figure 13. - Comparison of isentropic energy ratios using data measured by static-pressure probe at blade mean section and by end-wall static-pressure taps. Data measured 2.92 centimeters (1.15 in.) downstream of blading at nominal flow angle of 65° from axial, plane D (fig. 10); critical velocity ratio, 0.85 (approx.).

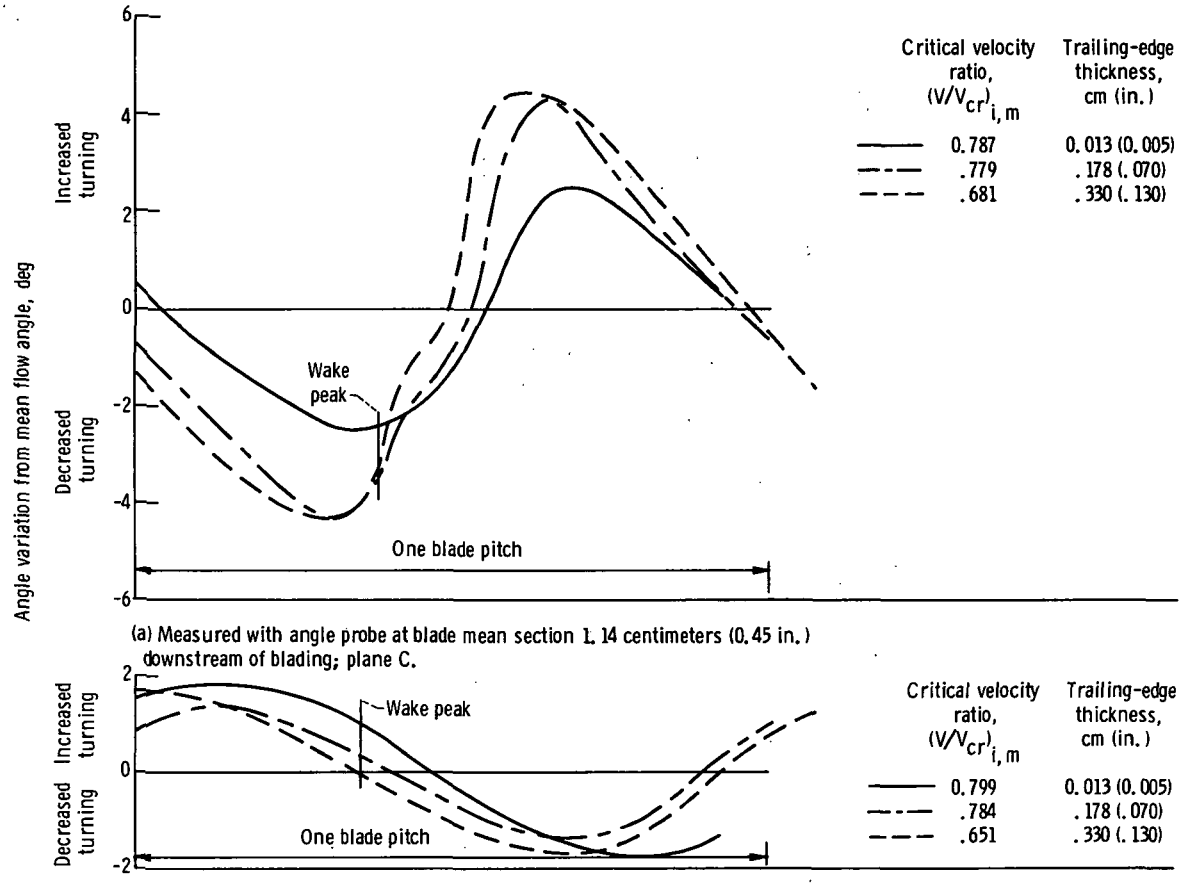

(a) Measured with angle probe at blade mean section 1.14 centimeters (0.45 in.) downstream of blading; plane C.

(b) Measured with angle probe at blade mean section 2.92 centimeters (1.15 in.) downstream of blading; plane D.

Figure 14. - Comparison of experimentally determined variations in flow angles for bladings with different round trailing-edge thickness at two downstream locations. Nominal flow angle, 65° from axial; trailing-edge thickness, 0.178 centimeter (0.070 in.).

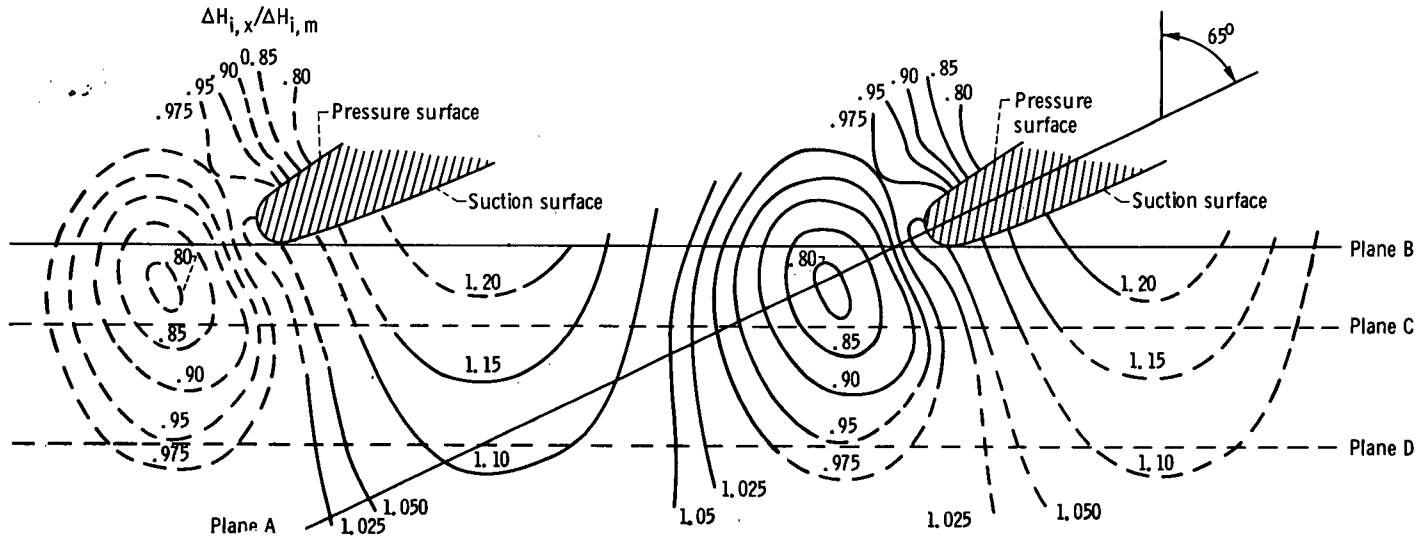

(a) Round trailing-edge thickness, 0.330 centimeter (0.130 in.).

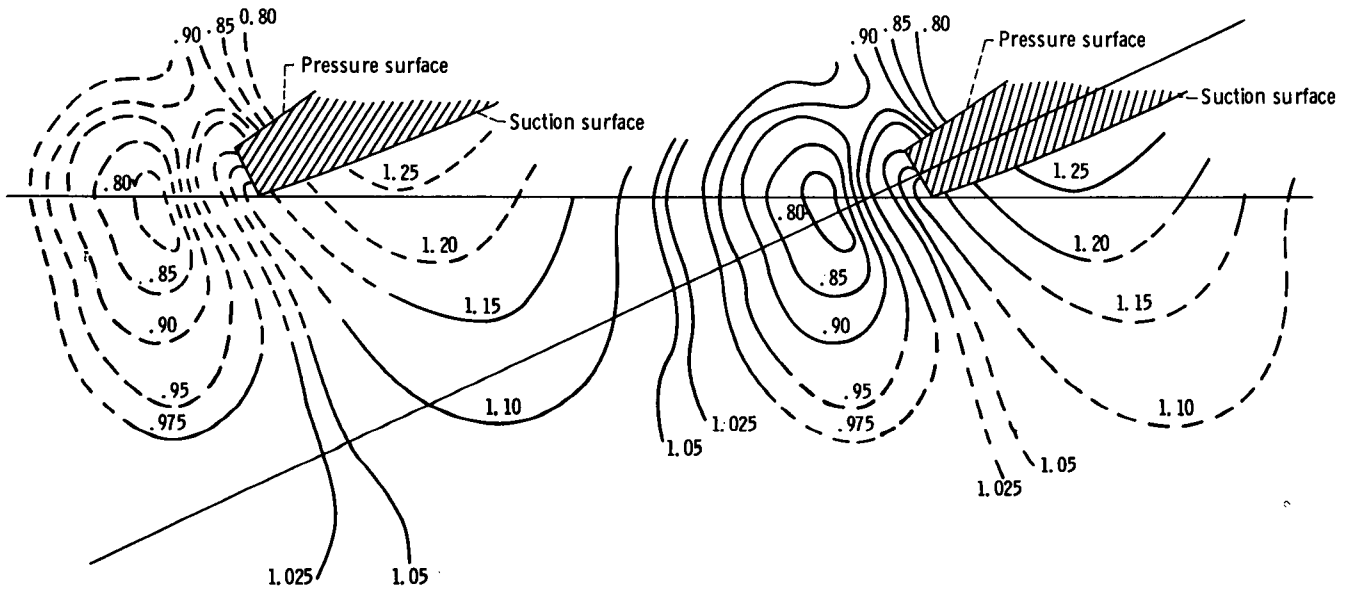

(b) Square trailing-edge thickness, 0.33 centimeter (0.130 in.).

Figure 15. - Comparison of isentropic energy ratios $\Delta H_{i,x}/\Delta H_{i,m}$ for blading with same trailing-edge thickness but different trailing-edge geometries. Ideal mixed critical velocity ratio, 0.85 (approx.); data measured by wall static-pressure taps.

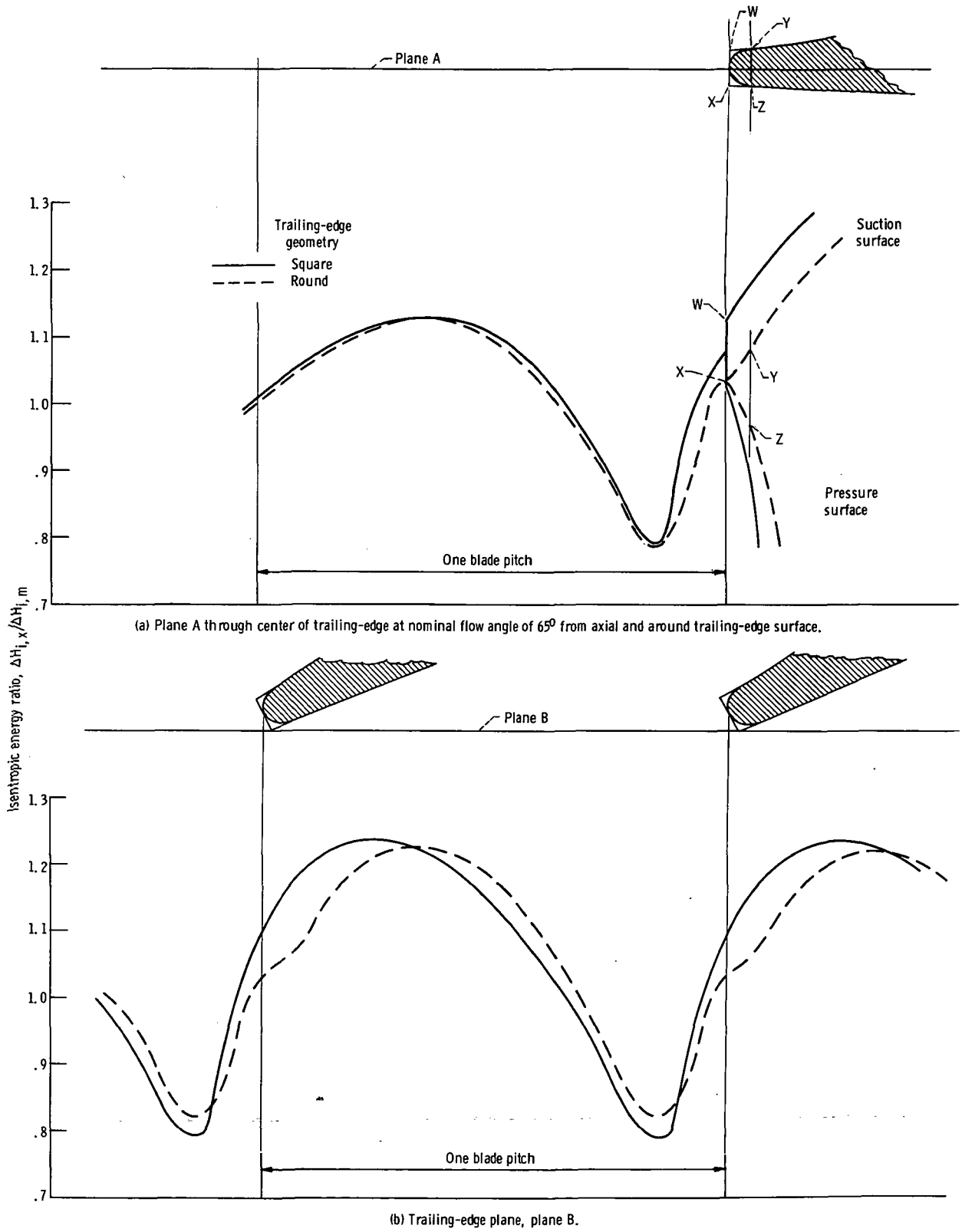

(a) Plane A through center of trailing-edge at nominal flow angle of 65^0 from axial and around trailing-edge surface.

(b) Trailing-edge plane, plane B.

Figure 16. - Comparison of isentropic energy ratios for blading with same trailing-edge thickness (0.330 cm (0.130 in.)) but different trailing-edge geometries in four planes and around trailing-edge surface. Data measured by wall static-pressure taps; ideal mixed critical velocity ratio, 0.85 (approx.).

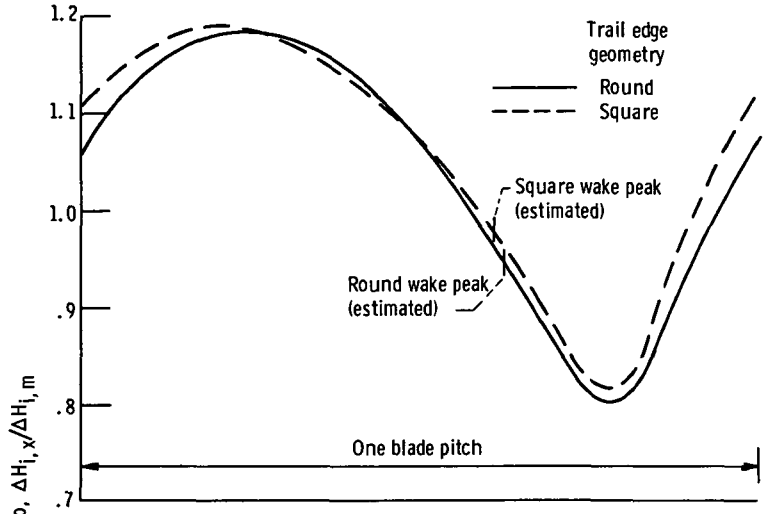

(c) Measured 1.14 centimeters (0.45 in.) downstream of blading at nominal flow angle of 65° from axial; plane C (fig. 15).

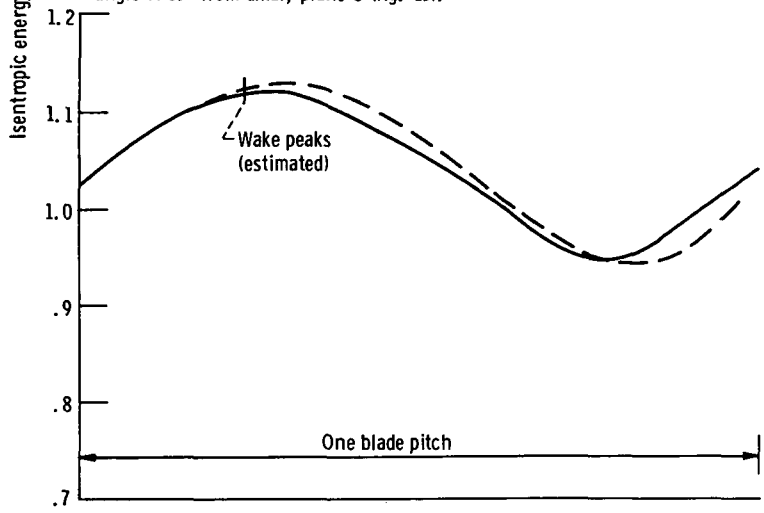

(d) Measured 2.92 centimeters (1.15 in.) downstream of blading at nominal flow angle of 65° from axial; plane D (fig. 15).

Figure 16. - Concluded.

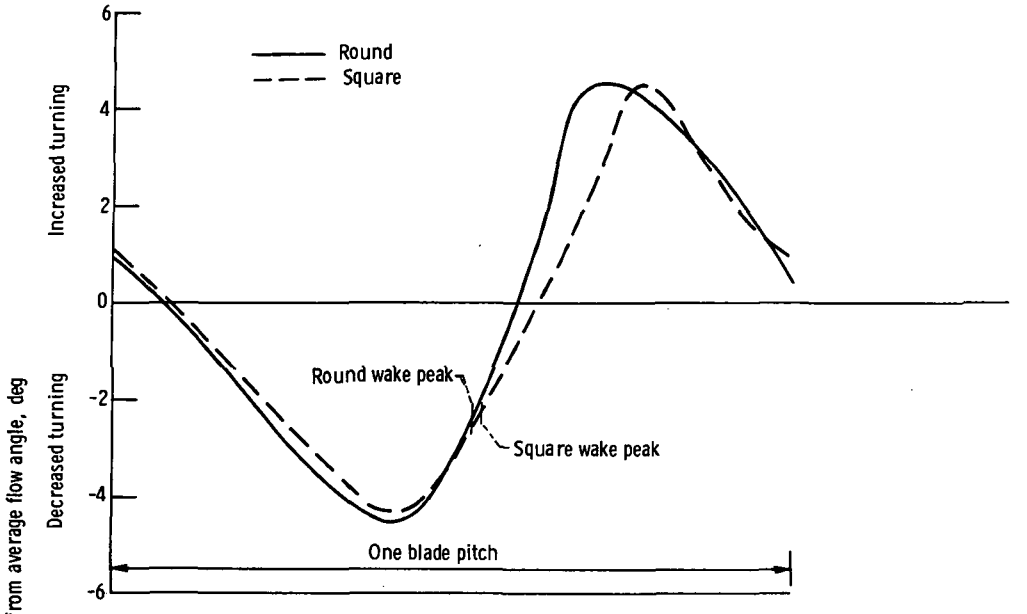

(a) Measured 1.14 centimeters (0.45 in.) downstream of blading in average flow direction; plane C (fig. 15); ideal mixed critical velocity ratio, 0.79 (approx.).

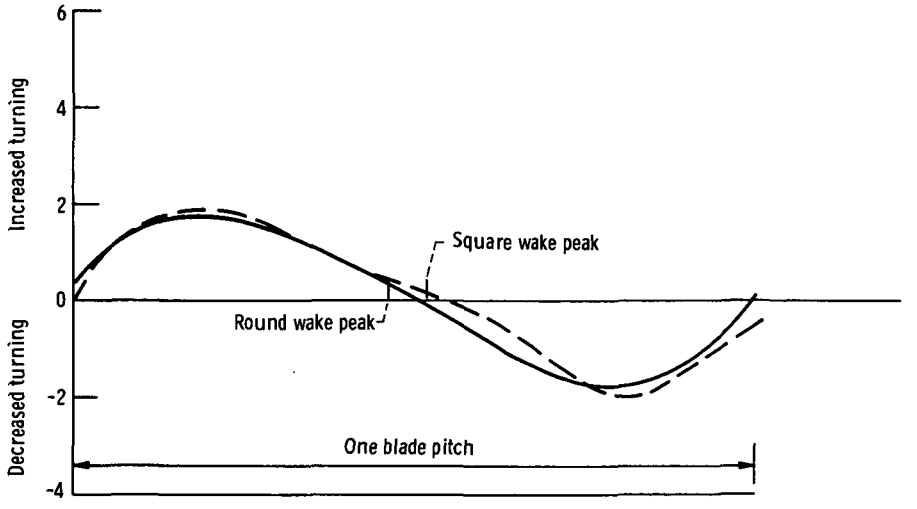

(b) Measured 2.92 centimeters (1.15 in.) downstream of blading in average flow direction; plane D (fig. 15); ideal mixed critical velocity ratio, 0.55 (approx.).

Figure 17. - Comparison of experimental flow angle variations in two different planes for blading with round and square trailing-edge geometries. Trailing-edge thickness, 0.330 centimeters (0.130 in.); data measured by angle probe at blade mean section.

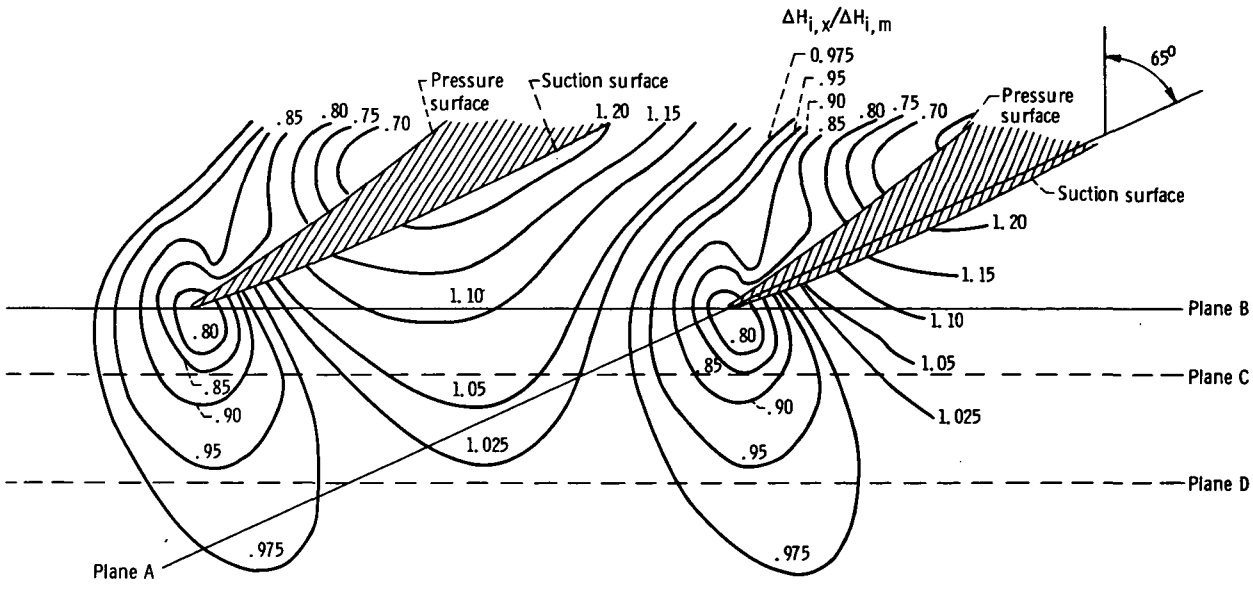

Analytical; ideal mixed critical velocity ratio, 0.79 (approx.)

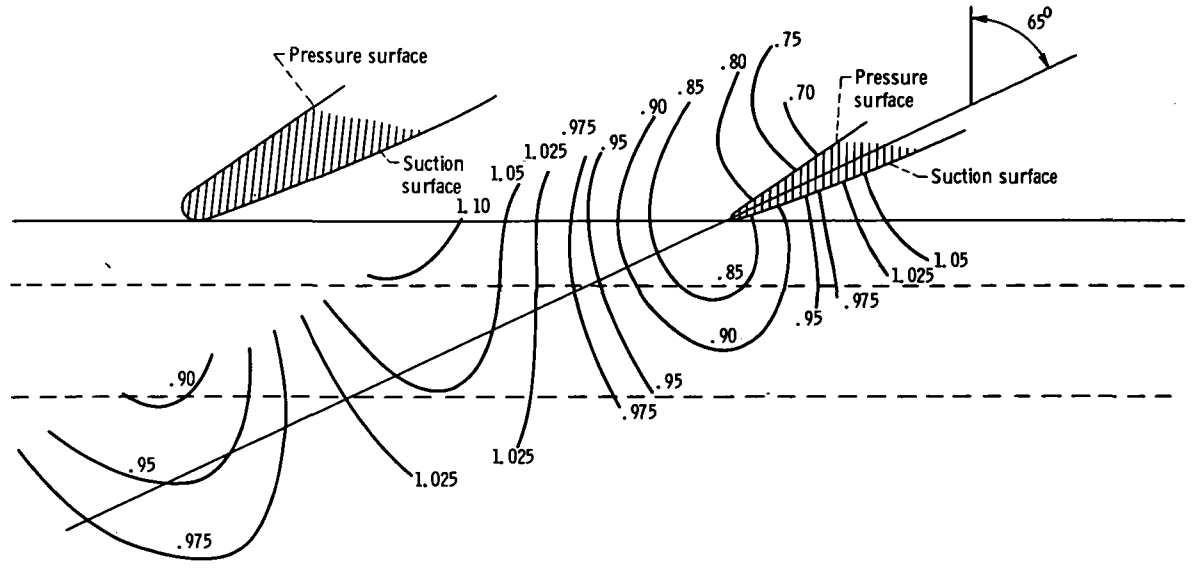

Experimental; ideal mixed critical velocity ratio, 0.85 (approx.)

(a) Trailing-edge thickness, 0.013 centimeter (0.005 in.).

Figure 18. - Comparison of experimental and analytically determined contours of isentropic energy ratios $\Delta H_{i,x}/\Delta H_{i,m}$ for three bladings with different round trailing-edge thicknesses. Experimental data determined by wall static-pressure taps.

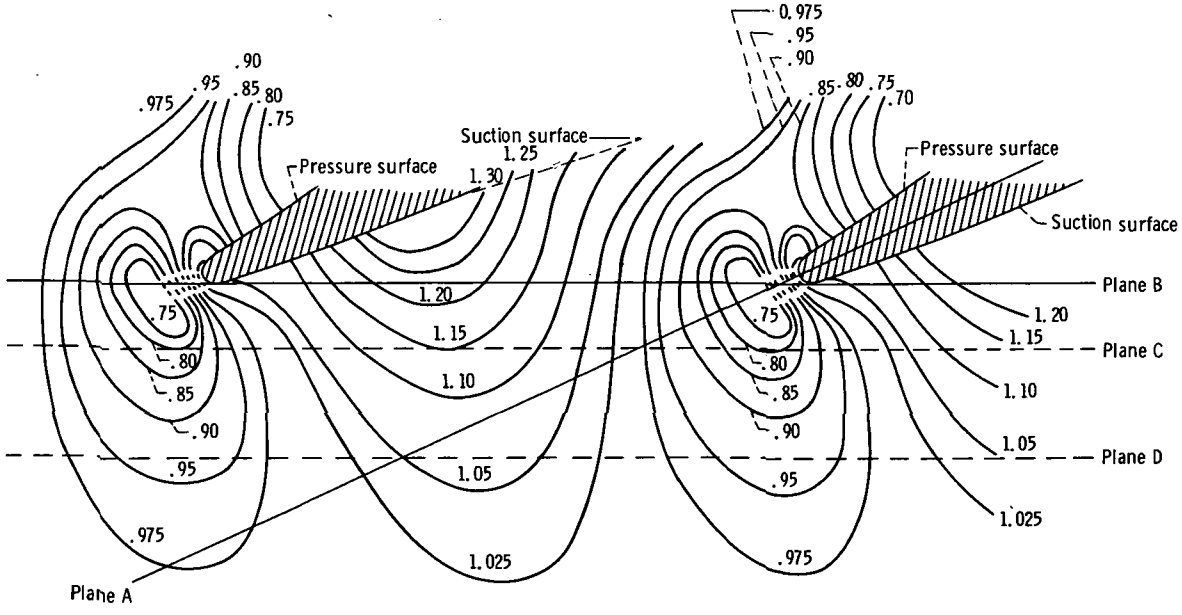

Analytical; ideal mixed critical velocity ratio, 0.78 (approx.)

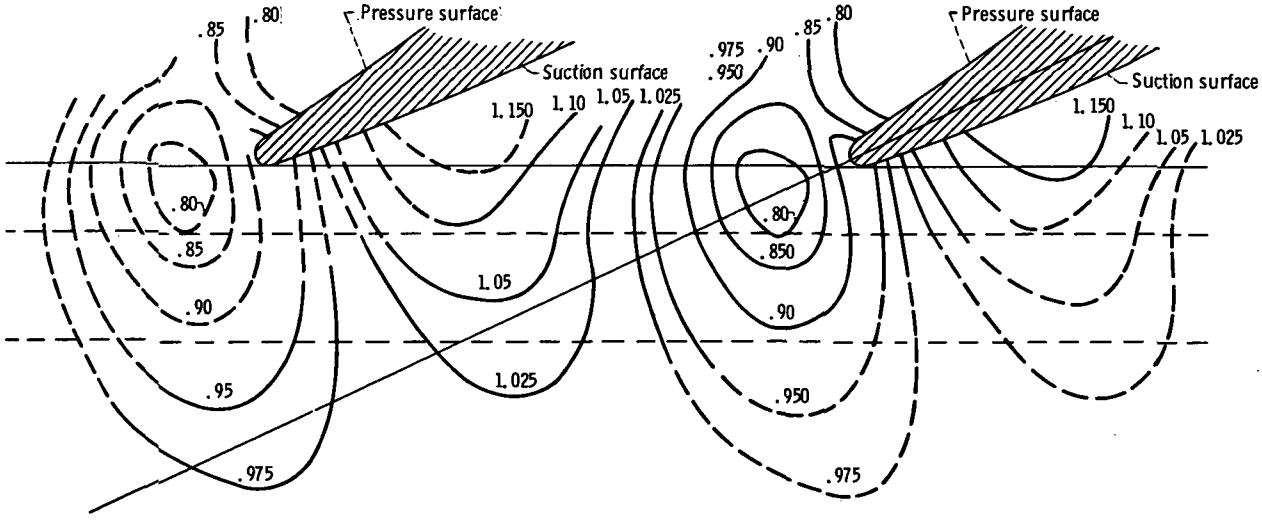

Experimental; ideal mixed critical velocity ratio, 0.8 (approx.)

(b) Trailing-edge thickness, 0.178 centimeter (0.070 in.).

Figure 18. - Continued.

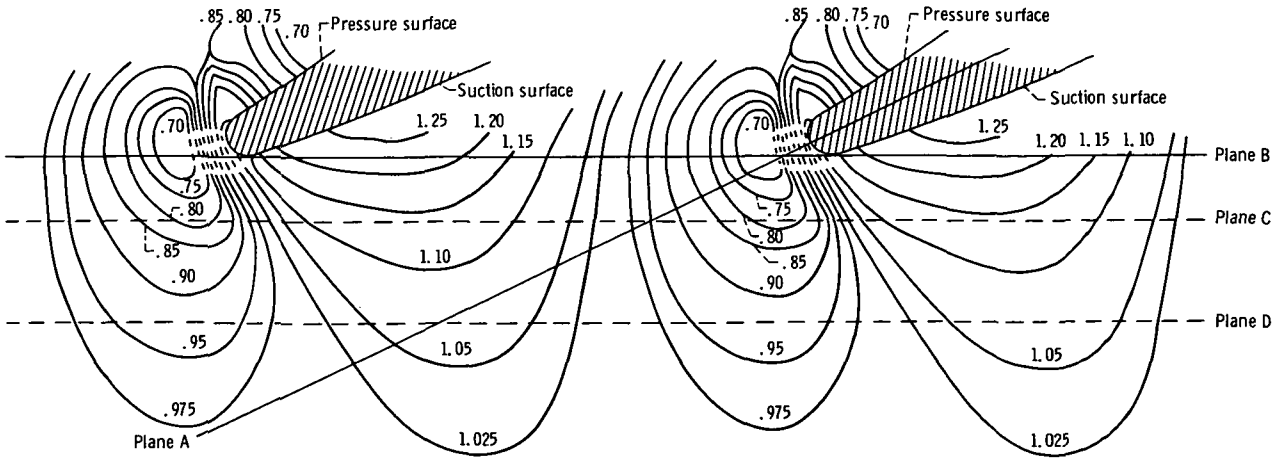

Analytical; ideal mixed critical velocity ratio, 0.70 (approx.)

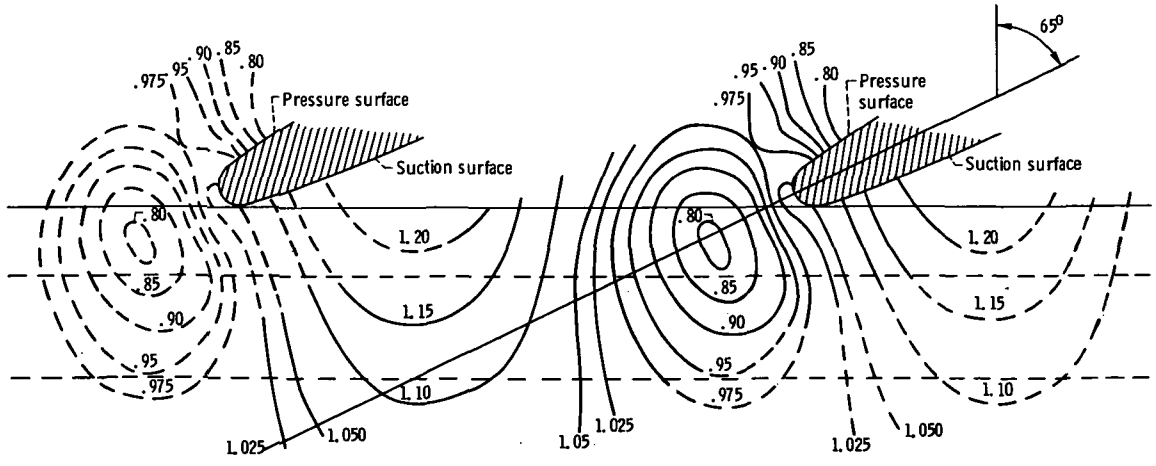

Experimental; ideal mixed critical velocity ratio, 0.85 (approx.)

(c) Trailing-edge thickness, 0.330 centimeter (0.130 in.).

Figure 18. - Concluded.

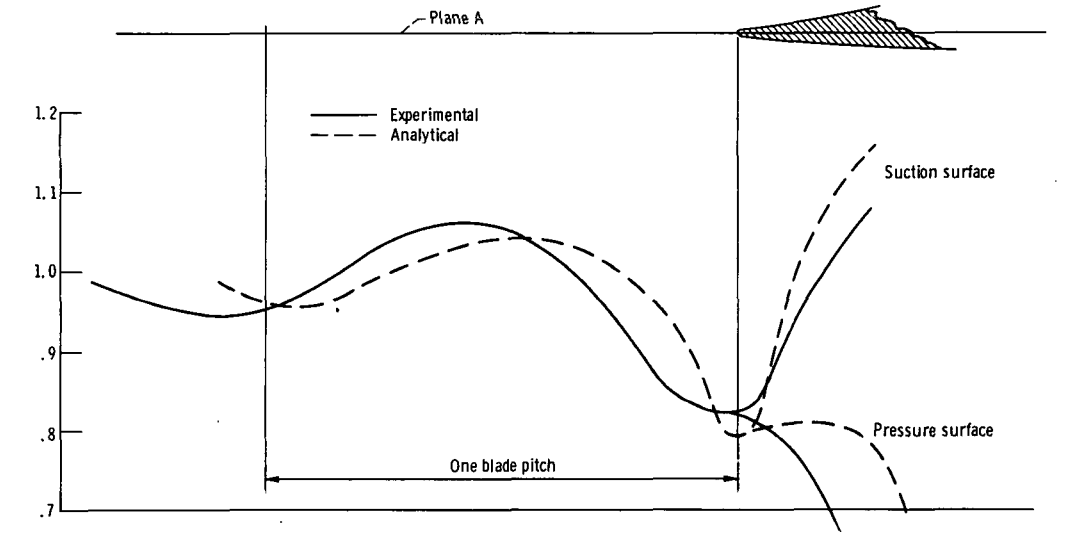

(a) Trailing-edge thickness, 0.013 centimeter (0.005 in.); analytical critical velocity ratio, 0.79.

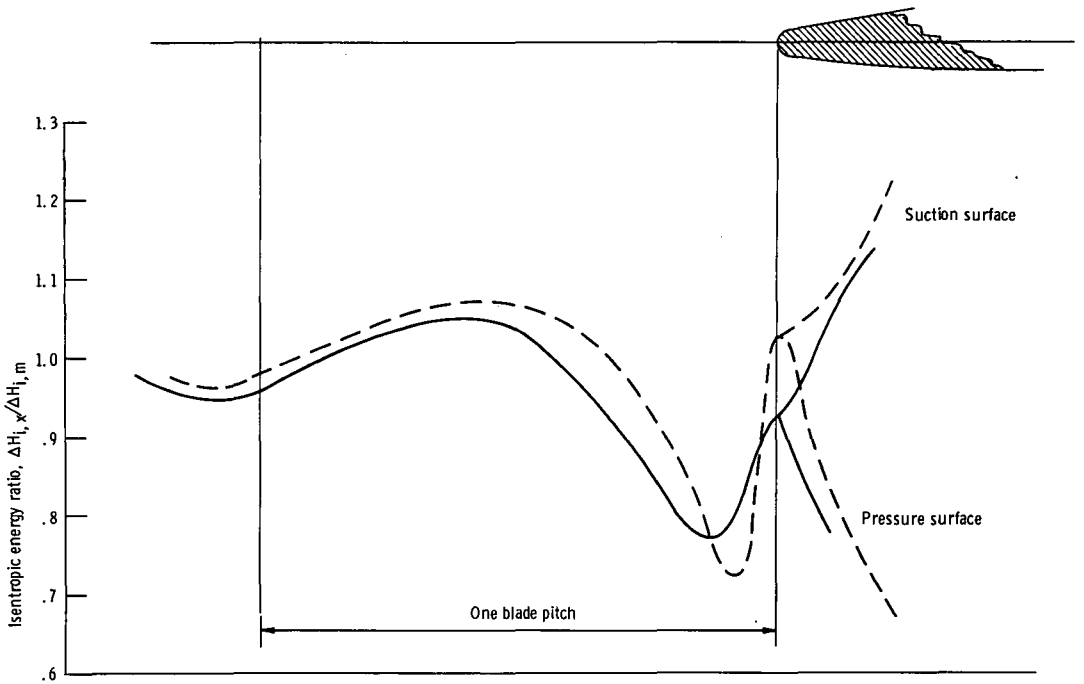

(b) Trailing-edge thickness, 0.178 centimeter (0.070 in.); analytical critical velocity ratio, 0.78.

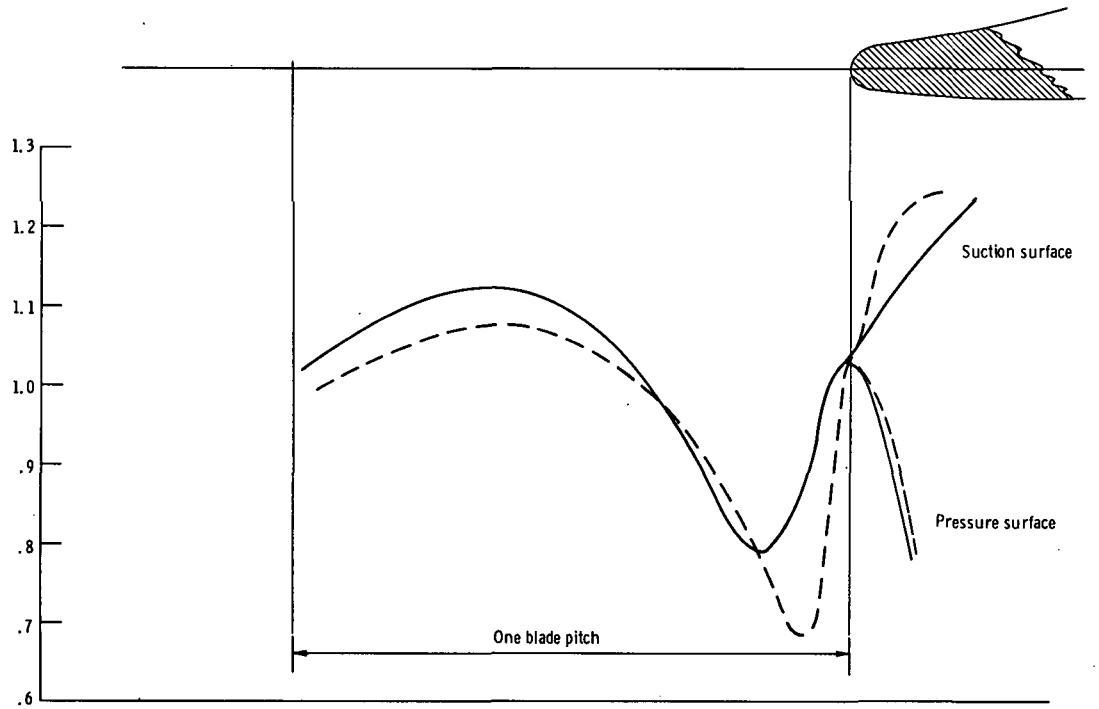

(c) Trailing-edge thickness, 0.330 centimeter (0.130 in.); analytical critical velocity ratio, 0.70.

Figure 19. - Comparisons of experimentally and analytically determined values of isentropic energy ratios for three bladings with different round trailing-edge thicknesses in plane through center of trailing edge at nominal flow angle of 65^0 from axial and around trailing-edge surface. Experimental data measured by wall static-pressure taps. Experimental critical velocity ratio, 0.85. (All critical velocity ratios are approximate.)

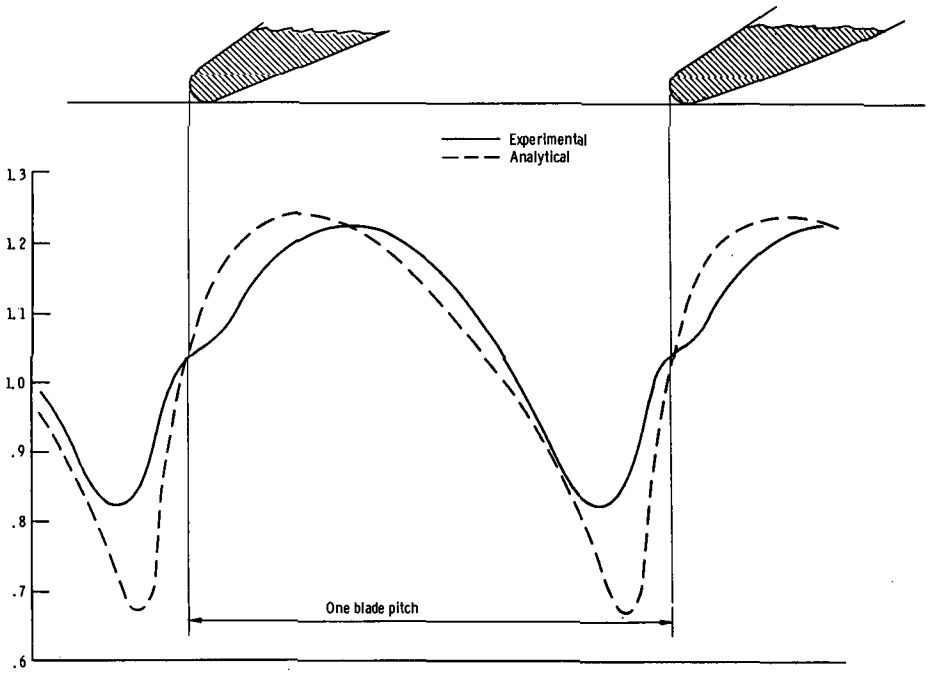

(a) Trailing-edge thickness, 0.013 centimeter (0.005 in.); analytical ideal mixed critical velocity ratio, 0.70.

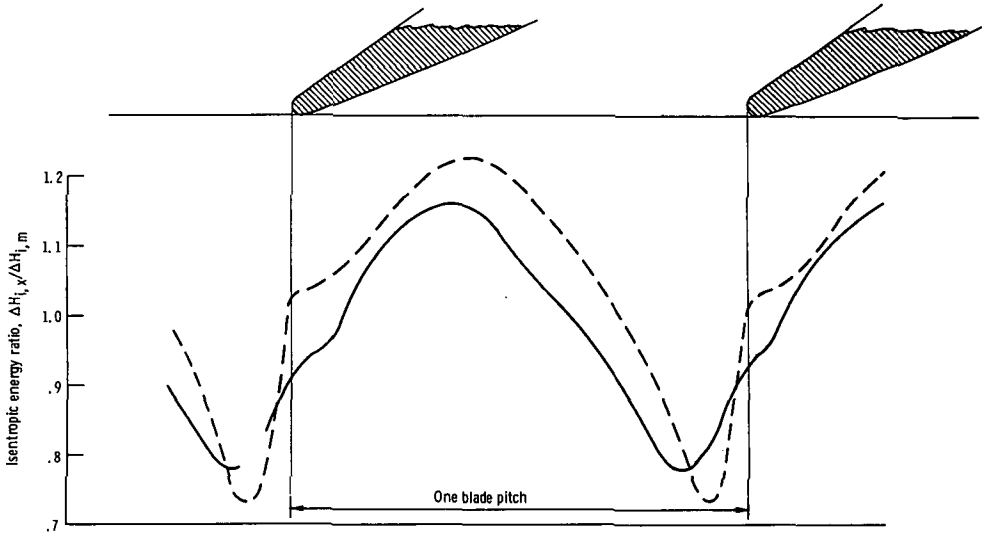

(b) Trailing-edge thickness, 0.178 centimeter (0.070 in.); analytical ideal mixed critical velocity ratio, 0.78.

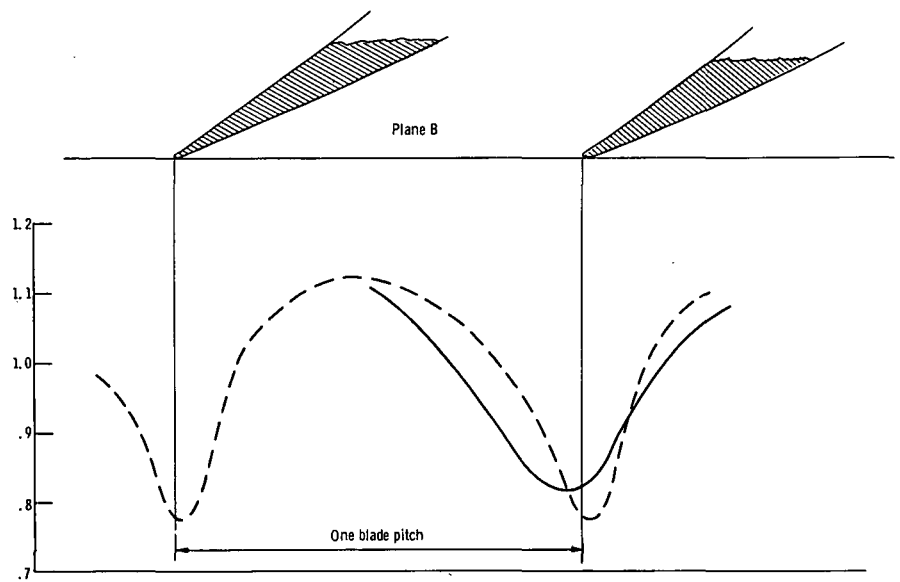

(c) Trailing-edge thickness, 0.330 centimeter (0.130 in.); analytical ideal mixed critical velocity ratio, 0.79.

Figure 20. - Comparison of experimentally and analytically determined values of isentropic energy ratios for three bladings with different round trailing-edge thicknesses in trailing-edge plane (plane B). Experimental critical velocity ratio, 0.85; experimental data determined by wall static-pressure taps. (All critical velocity ratios are approximate.)

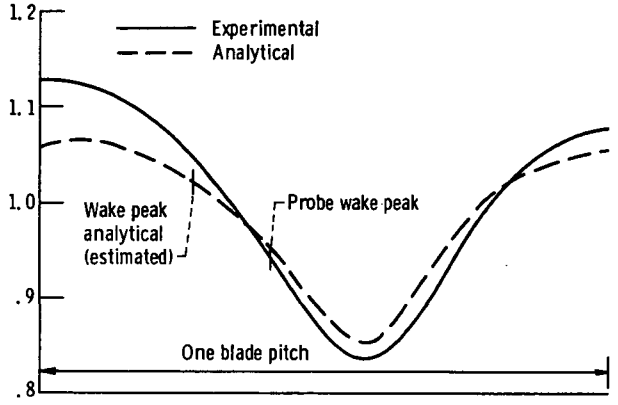

(a) Trailing-edge thickness 0.013 centimeter (0.005 in.); ideal mixed critical velocity ratio, 0.79 (approx.).

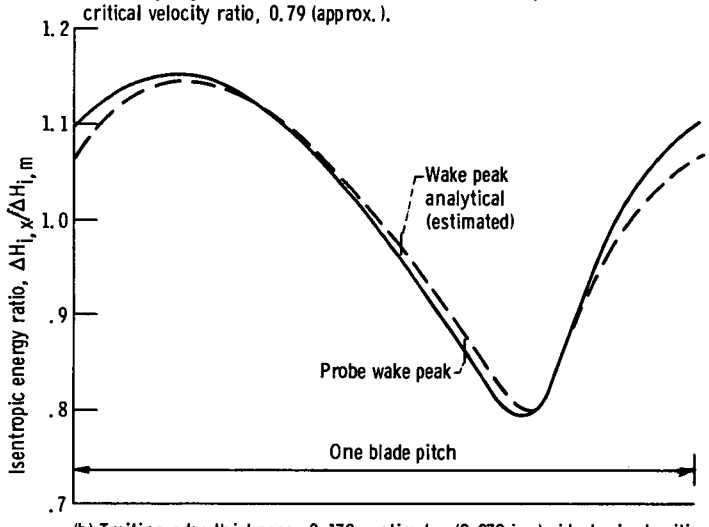

(b) Trailing-edge thickness, 0.178 centimeter (0.070 in.); ideal mixed critical velocity ratio, 0.78 (approx.).

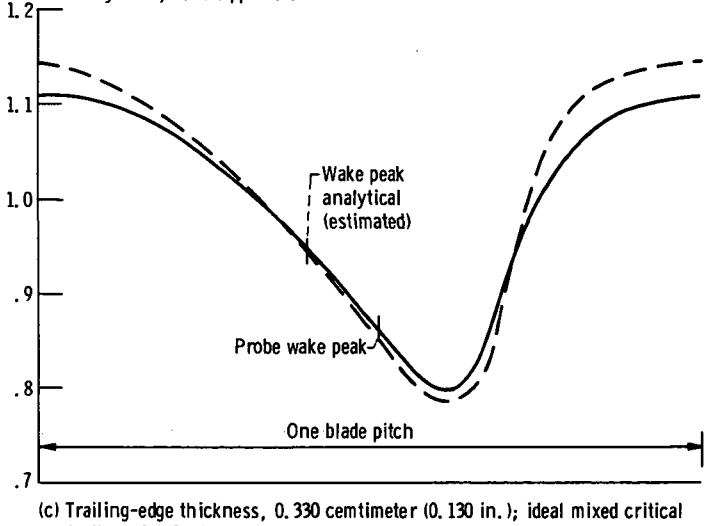

(c) Trailing-edge thickness, 0.330 cemtimeter (0.130 in.); ideal mixed critical velocity ratio, 0.70 (approx.).

Figure 21. - Comparison of experimentally and analytically determined values of isentropic energy ratios for three bladings with different round trailing-edge thickness in plane 1.14 centimeters (0.45 in.) downstream of blading at nominal flow angle of 65^{0} from axial.

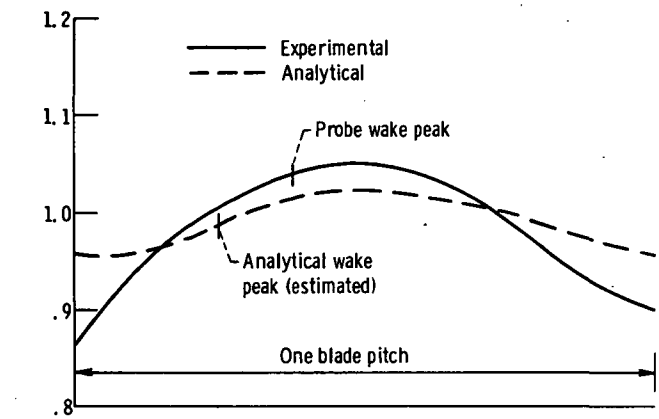

(a) Trailing-edge thickness, 0.015 centimeter (0.005 in.); experimental and analytical ideal mixed critical velocity ratio, 0.79.

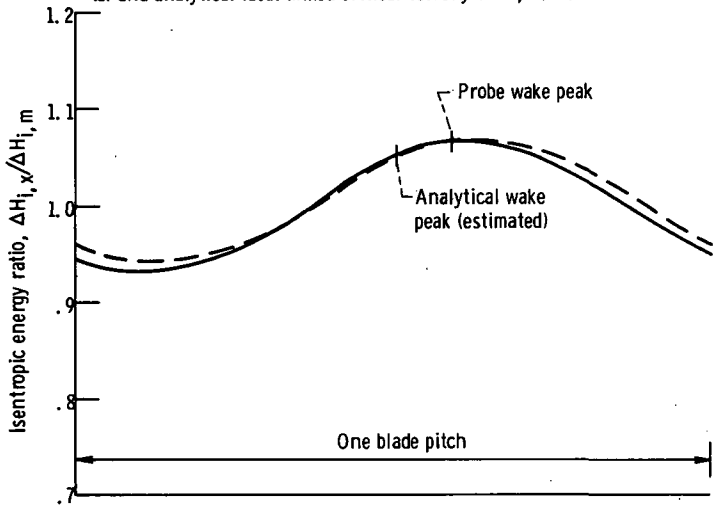

(b) Trailing-edge thickness, 0.178 centimeter (0.070 in.); experimental and analytical ideal mixed critical velocity ratio, 0.78.

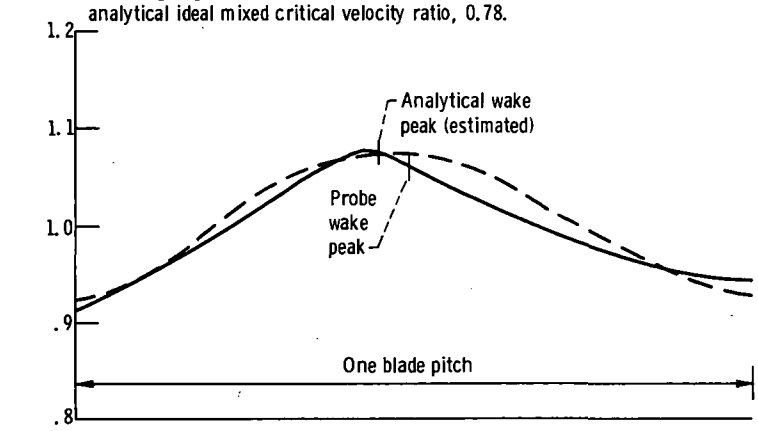

(c) Trailing-edge thickness, 0.330 centimeter (0.130 in.); ideal mixed critical velocity ratios: experimental, 0.70; analytical, 0.68.

Figure 22. - Comparison of experimentally and analytically determined values of isentropic energy ratios for three bladings with different round trailing-edge thicknesses in plane 2.92 centimeters (1.15 in.) downstream of blading at nominal flow angle of 65^0 from axial. (All critical velocity ratios are approximate.)

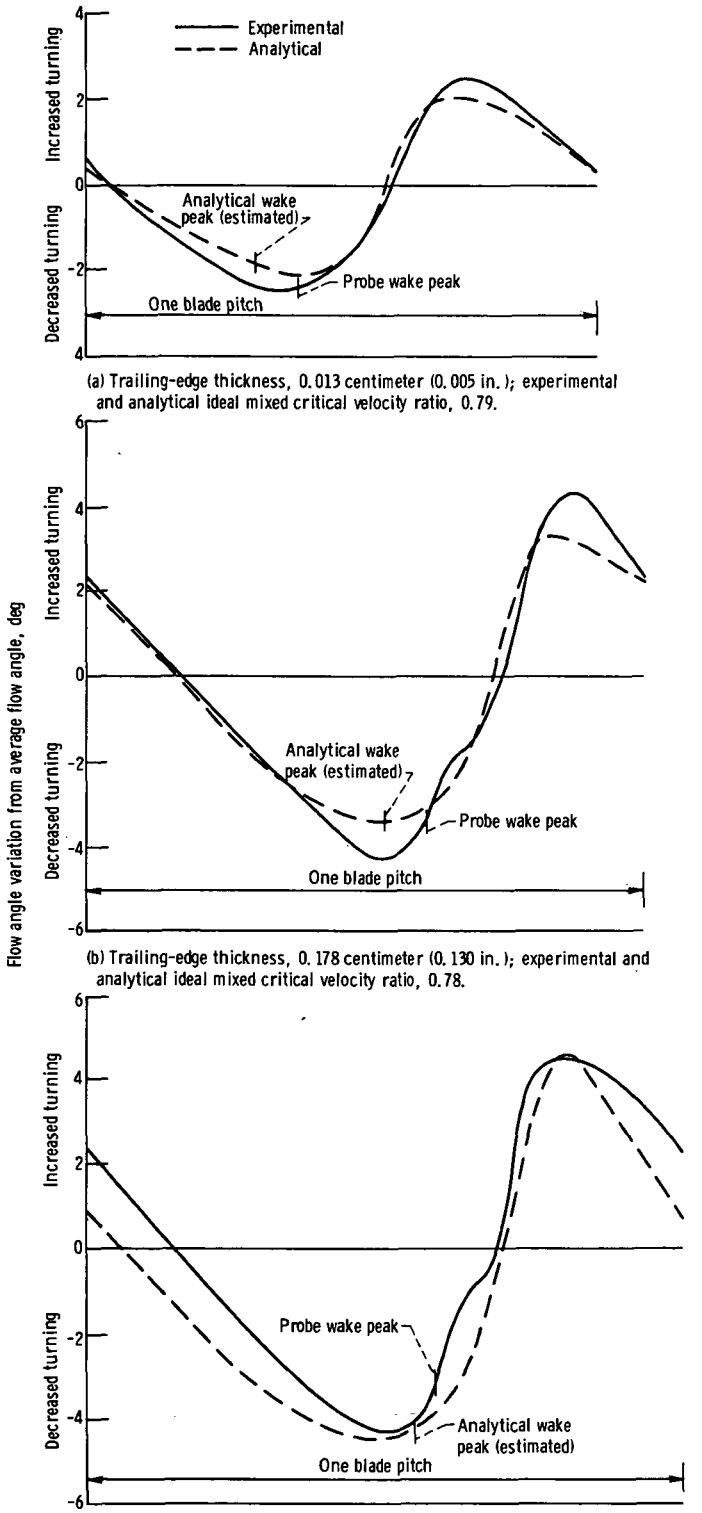

(a) Trailing-edge thickness, 0.013 centimeter (0.005 in.); experimental and analytical ideal mixed critical velocity ratio, 0.79.

(b) Trailing-edge thickness, 0.178 centimeter (0.130 in.); experimental and analytical ideal mixed critical velocity ratio, 0.78.

(c) Trailing-edge thickness, 0.330 centimeter (0.130 in); ideal mixed critical velocity ratios; experimental, 0.69; analytical, 0.70.

Figure 23. - Comparisons of experimentally and analytically determined variations in flow angle for three bladings with different round trailing-edge thicknesses in plane 1, 14 centimeters (0.45 in.) downstream of blading at nominal flow angle of 65^{0} from axial; plane C. (All critical velocity ratios are approximate.)

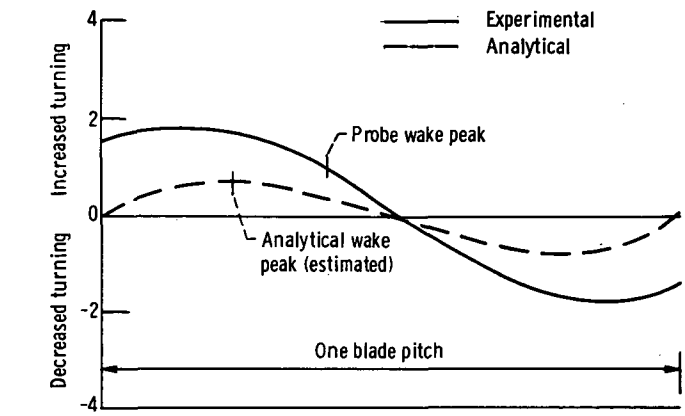

(a) Trailing-edge thickness, 0.013 centimeter (0.005 in.); experimental and analytical ideal mixed critical velocity ratio, 0.79.

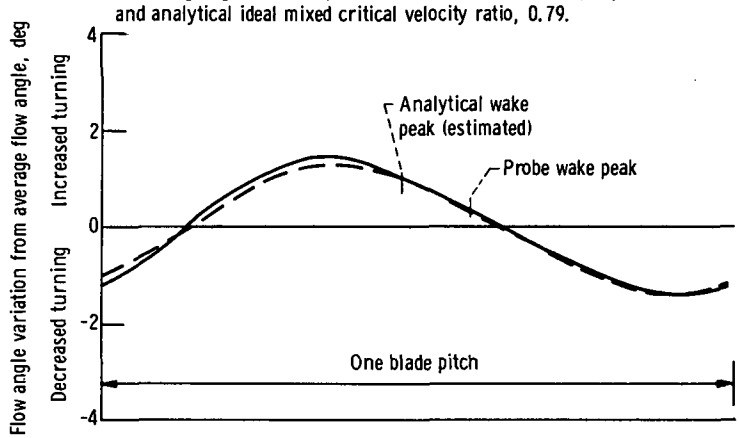

(b) Trailing-edge thickness, 0.178 centimeter (0.070 in.); experimental and analytical ideal mixed critical velocity ratio, 0.78.

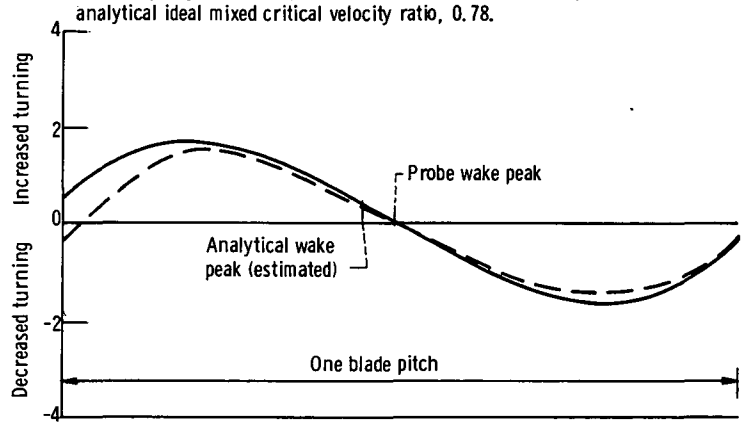

(c) Trailing-edge thickness, 0.330 centimeter (0.130 in.); ideal mixed critical velocity ratio; experimental, 0.66; analytical, 0.70.

Figure 24. - Comparison of experimentally and analytically determined variations in flow angle for three bladings with different round trailing-edge thicknesses in plane 2.92 centimeters (1.15 in.) downstream of blading at nominal flow angle of 65^{0} from axial; plane D (fig. 15).

NATIONAL AERONAUTICS AND SPACE ADMINISTRATION
WASHINGTON, D.C. 20546

OFFICIAL BUSINESS
PENALTY FOR PRIVATE USE $300

SPECIAL FOURTH-CLASS RATE
BOOK

POSTAGE AND FEES PAID
NATIONAL AERONAUTICS AND
SPACE ADMINISTRATION
451

U.S.MAIL

POSTMASTER: If Undeliverable (Section 158 Postal Manual) Do Not Return

"The aeronautical and space activities of the United States shall be conducted so as to contribute . . . to the expansion of human knowledge of phenomena in the atmosphere and space. The Administration shall provide for the widest practicable and appropriate dissemination of information concerning its activities and the results thereof."

—NATIONAL AERONAUTICS AND SPACE ACT OF 1958

NASA SCIENTIFIC AND TECHNICAL PUBLICATIONS

TECHNICAL REPORTS: Scientific and technical information considered important, complete, and a lasting contribution to existing knowledge.

TECHNICAL NOTES: Information less broad in scope but nevertheless of importance as a contribution to existing knowledge.

TECHNICAL MEMORANDUMS: Information receiving limited distribution because of preliminary data, security classification, or other reasons. Also includes conference proceedings with either limited or unlimited distribution.

CONTRACTOR REPORTS: Scientific and technical information generated under a NASA contract or grant and considered an important contribution to existing knowledge.

TECHNICAL TRANSLATIONS: Information published in a foreign language considered to merit NASA distribution in English.

SPECIAL PUBLICATIONS: Information derived from or of value to NASA activities. Publications include final reports of major projects, monographs, data compilations, handbooks, sourcebooks, and special bibliographies.

TECHNOLOGY UTILIZATION PUBLICATIONS: Information on technology used by NASA that may be of particular interest in commercial and other non-aerospace applications. Publications include Tech Briefs, Technology Utilization Reports and Technology Surveys.

Details on the availability of these publications may be obtained from:

SCIENTIFIC AND TECHNICAL INFORMATION OFFICE

NATIONAL AERONAUTICS AND SPACE ADMINISTRATION

Washington, D.C. 20546